Copyright Warning & Restrictions

The copyright law of the United States (Title 17, United States Code) governs the making of photocopies or other reproductions of copyrighted material.

Under certain conditions specified in the law, libraries and archives are authorized to furnish a photocopy or other reproduction. One of these specified conditions is that the photocopy or reproduction is not to be "used for any purpose other than private study, scholarship, or research." If a, user makes a request for, or later uses, a photocopy or reproduction for purposes in excess of "fair use" that user may be liable for copyright infringement,

This institution reserves the right to refuse to accept a copying order if, in its judgment, fulfillment of the order would involve violation of copyright law.

Please Note: The author retains the copyright while the New Jersey Institute of Technology reserves the right to distribute this thesis or dissertation

Printing note: If you do not wish to print this page, then select "Pages from: first page # to: last page #" on the print dialog screen

ABSTRACT

RESONANT TRIAD INTERACTIONS IN ONE AND TWO-LAYER SYSTEMS

by
Malik Chabane

This dissertation is a study of the weakly nonlinear resonant interactions of a triad of gravity-capillary waves in systems of one and two fluid layers of arbitrary depth, in one and two-dimentions. For one-layer systems, resonant triad interactions of gravity-capillary waves are considered and a region where resonant triads can be always found is identified, in the two-dimensional wavevector angles-space. Then a description of the variations of resonant wavenumbers and wave frequencies over the resonance region is given. The amplitude equations correct to second order in wave slope are used to investigate special resonant triads that, providing their initial amplitude and relative phase satisfy appropriate conditions, exchange no energy during their interactions, which implies that the wave amplitudes remain constant in time. From the fact that the steadiness of the wave amplitudes is a necessary condition for resonant triads to form traveling waves, a transversely modulated two-dimensional wave field of permanent form is found and can be considered as a generalization of Wilton ripples. For two-layer systems, resonant triad interactions between surface and interfacial gravity waves propagating in two horizontal dimensions are considered. As the system supports both surface and internal wave modes, two different types of resonant triad interactions are possible: one with two surface and one internal wave modes and the other with one surface and two internal wave modes. Presented are the spectral domains, where, for given physical parameters, the two resonance scenarios can be found. It is shown that one-dimensional triads occur on the boundary of the spectral domain of resonance. Using a set of amplitude equations recently derived by Choi et al, [10], the necessary and sufficient conditions to form traveling waves are

found when the three wave trains travel in the same directions (class-III and class-IV resonance). In addition, a set of physical parameters for one-dimensional triads, for which these traveling waves are possible, is presented.

RESONANT TRIAD INTERACTIONS IN ONE AND TWO-LAYER SYSTEMS

by
Malik Chabane

A Dissertation
Submitted to the Faculty of
New Jersey Institute of Technology and
Rutgers, The State University of New Jersey – Newark
in Partial Fulfillment of the Requirements for the Degree of
Doctor of Philosophy in Mathematical Sciences

Department of Mathematical Sciences
Department of Mathematics and Computer Science, Rutgers-Newark

August 2020

APPROVAL PAGE

RESONANT TRIAD INTERACTIONS IN ONE AND TWO-LAYER SYSTEMS

Malik Chabane

Wooyoung Choi, Dissertation Advisor — Date
Professor of Mathematics, New Jersey Institute of Technology

Diane M. Henderson, Committee Member — Date
Professor of Mathematics, Pennsylvania State University

Roy H. Goodman, Committee Member — Date
Associate Professor of Mathematics, New Jersey Institute of Technology

---

Richard O. Moore, Committee Member — Date
Director of Programs and Services, Society for Industrial and Applied Mathematics

---

David Shirokoff, Committee Member — Date
Assistant Professor of Mathematics, New Jersey Institute of Technology

BIOGRAPHICAL SKETCH

Author: Malik Chabane

Degree: Doctor of Philosophy

Date: August 2020

Undergraduate and Graduate Education:

- Doctor of Philosophy in Mathematical Sciences,
  New Jersey Institute of Technology, Newark, NJ, 2020
- Master of Science in Fluid Dynamics
  Paul Sabatier University, Toulouse, France, 2013
- Bachelor of Science Mechanics
  Paul Sabatier University, Toulouse, France, 2011

Major: Mathematical Sciences

Presentations and Publications:

W. Choi, M. Chabane, T. M. A. Taklo, Two-dimensional resonant triad interactions in a two-layer system, *Submitted to Journal of Fluid Mechanics*, 2020.

M. Chabane, W. Choi, On resonant interactions of gravity-capillary waves without energy exchange, *Studies in Applied Mathematics*, 142:528-550, 2019.

M. Chabane, A. Tur, V. Yanovsky, Saturation of a large scale instability and non linear structures in a rotating stratified flow, *arXiv: 1406. 3962*, 2014.

M. Chabane, A. Tur, V. Yanovsky, A new large scale instability in rotating stratified fluids driven by small scale forces, *Open Journal of Fluid Dynamics*, 3, 340-351, 2013.

I dedicate my dissertation work to my family.

ACKNOWLEDGMENT

First of all, I would like to express my deepest gratitude to my advisor Prof. Wooyoung Choi. I could not thank him enough for the continuous support he gave me. Only his kindness matches up to his patience. I could not have imagined having a better advisor and mentor for my Ph.D. studies.

Besides my advisor, I would like to thank the rest of my thesis committee: Prof. Richard Moore, Prof. Roy Goodman, Prof. David Shirokoff and Prof. Diane Henderson. Thank you for your availability and your kindness.

My sincere thanks also go to the department of Mathematical Sciences, who provided me an opportunity to join their graduate program and who supported me financially throughout these years. Thank you to Linda Cummings who was in charge of the graduate program at that time, and to all of the department staff.

If those years have been an unforgettable part of my life, it is also thanks to the great friends I made. Thank you Andrew, Matt, Mahdi and RJ. Thank you to Dave, Jimmie, Axel, Tore, Connor, and Brandon.

Last, but not least, I would like to thank my family: my beloved parents, my brother (who, while I was working on *capillary*-waves, genuinely believed, until recently, that I was studying hairs), my sister and my family-in-law, for their unconditional love and support. I want to thank my dear wife for her support, her patience, and the constant happiness she put into our life no matter what the situation was; and finally, I want to thank my children, who, without even knowing it, have been the main source of my strength all along.

TABLE OF CONTENTS

TABLE OF CONTENTS
(Continued)

Chapter **Page**

LIST OF FIGURES

Figure **Page**

LIST OF FIGURES
(Continued)

Figure **Page**

LIST OF FIGURES
(Continued)

Figure **Page**

CHAPTER 1

INTRODUCTION

Resonant interactions of weakly nonlinear waves on the surface of water have been considered one of main mechanisms for the long-term evolution of wave spectrum (Hammack and Henderson [13]). In 1960, Owen Martin Phillips, inspired by energy exchanges in turbulence due to nonlinearities [23], was the first to discover the nonlinear resonant interactions of gravity waves. He showed [22] that resonant interactions between three gravity waves are impossible and that the first interactions appear among quadruplets at the third order in wave slope. This new phenomenon was first experimentally confirmed by Longuet-Higgins and Smith [18] and McGoldrick et al, [20]. In 1962, Benney [3] derived a complete set of interaction equations for the wave amplitudes. On the other hand, Simmons [25] showed that the amplitude equation can also be obtained through a variational formulation. While it can be neglected for surface waves of relatively long wavelengths, the surface tension must be included for short waves of a few centimeters or less. McGoldrick [19] later showed that three-waves resonance is possible at the second order if surface tension effects are included, and that the solutions of the amplitude equations can be written in terms of Jacobian elliptic functions. In general, the resonant triad exchanges their energies (proportional to $|A_j|^2$ with $A_j = |A_j|\exp(i\varphi_j)$) periodically in time while the total energy is conserved in the absence of viscosity. This has also been confirmed by laboratory experiments (see the review of Hammack and Henderson [13]. Later on, McGoldrick [21] showed that Wilton ripples [28] are in fact a result of the resonant interaction of a particular wavenumber with its second harmonic.

For two-layer systems, it is well known that three-wave resonant interactions are possible between surface and internal gravity waves at second-order nonlinearity, even in the absence of surface tension. Nonlinear resonant interactions between surface

and internal waves have been studied mostly for one-dimensional waves. Ball [2] gave a detailed analysis of the shallow water case where two counter-propagating surface waves and on internal wave are involved (so-called class-I resonance). Hill & Foda [14] conducted laboratory experiments of counter-propagating internal waves interacting with one surface wave (class-II), which has been described more formally by Segur [24]. Joyce [15] provided experimental results of two standing surface waves that interact with one internal wave. Alam [1] used a geometrical argument to show the possibility of resonance between two co-propagating surface waves along with one internal wave which he referred to as class-III resonance. Although this work will focus on traveling waves for by triads (waves of steady amplitudes), it is worth mentioning that class-III resonance is relevant to ocean waves, for example as a model to describe the mechanism of short surface wave modulation by long internal waves, the class-III resonance has been studied for a few decades both experimentally and theoretically for progressive waves (Lewis et al. [17]; Alam [1]; Tanaka and Wakayama [27]; Taklo and Choi [26]) and for standing waves (Joyce [15]). In addition, the critical case of the class-III resonance where the internal wavenumber approaches zero has been investigated for its possible application to surface expressions of internal solitary waves (Hashizume [12]; Funakoshi and Oikawa [11]; Kodaira et al. [16]). Alam [1] mentioned for strong density ratio (hence, not realistic in the ocean), the existence of another class of resonance (which we will call class-IV) that involves two co-propagating internal waves and one surface wave. While 1D resonant interactions have been previously investigated, their generalization to two-dimensional (2D) waves has been limited to a few special cases. In particular, no general description of the regions of resonance between surface and internal waves of arbitrary wavelength have been provided. For two-dimensional waves, it seems more relevant to classify triad resonance into two groups: those involving two surface waves and those involving two internal waves. In that case, class-I and class-III belong to the same group and are

distinguished by the angle between the waves.

This work is organized as follows. After presenting the mathematical formulation of the triad resonance problem in §2, we discuss in §3 one-layer systems for which we reexamine 1D and 2D resonances in the gravity-capillary regime with a focus on three waves that exchange no energy during their interaction. Given surface and internal wave modes, two types of triad resonance are possible. The first consists of two surface waves interacting with one internal wave which will be referred to as type-A, and the other consists of one surface wave interacting with two internal waves which will be called type-B. Chapter §4 is devoted to two-layer systems, where we present regions in spectral space, where resonant interactions of two-dimensional triad occur for both type-A and type-B resonance. In §4.4, we focus on one-dimensional waves, and present general conditions for traveling wave solutions by matching linear wave speeds and nonlinear corrections separately. It is shown that without surface tension, traveling wave solutions are available only for class-IV resonance. In §4.5, we show how the surface tension affects the resonance regions, and traveling wave solutions in class-III resonance. We will conclude with some remarks in §5.

CHAPTER 2

MATHEMATICAL FORMULATION

2.1 Nonlinear Resonance

Nonlinear resonance refers to the phenomenon in which natural frequencies of a system are excited by its own nonlinearities, as opposed to an external forcing in the case of linear resonance. Consider the following general form for a PDE

$$L[u] + N[u] = 0 \tag{2.1}$$

where L and N are linear and nonlinear operators respectively. Consider a small parameter $\epsilon \ll 1$ of the system and expand u as a power series:

$$u = \sum_{n=1}^{\infty} \epsilon^n u_n. \tag{2.2}$$

Substituting (2.2) to (2.1) and regrouping in power of ϵ yield the system

$$L[u_1] = 0, \tag{2.3}$$

$$L[u_2] = N^{(2)}[u_1], \tag{2.4}$$

$$L[u_3] = N^{(2)}[u_1, u_2] + N^{(3)}[u_1, u_1, u_1], \tag{2.5}$$

and so on, where $N^{(n)}$ is the nonlinear operator of u generating n^{th} degree products. At $\mathcal{O}(\epsilon)$, equation (2.3) is linear and, in the case of triad interaction, the linear

solution is sought in the form of

$$u_1 = \sum_{j=1}^{3} A_j \mathrm{e}^{\mathrm{i}\Theta_j} + A_j^* \mathrm{e}^{-\mathrm{i}\Theta_j}, \tag{2.6}$$

where $\Theta_j = \boldsymbol{k}_j \cdot \boldsymbol{x} - \omega_j t$, $\boldsymbol{k}_j$ are the wave vectors, ω_j are the frequencies, $\boldsymbol{x}$ the position vector, and t is the time. This solution is associated with a dispersion relation

$$\omega = W(\boldsymbol{k}). \tag{2.7}$$

Substituting (2.6) in the right-hand side of (2.4) will generate nonlinear interactions between different wave trains, and, secular terms arise if

$$\boldsymbol{k}_1 = \boldsymbol{k}_2 + \boldsymbol{k}_3\,, \qquad \omega_1 = \omega_2 + \omega_3\,, \qquad \omega_j = W(\boldsymbol{k}_j). \tag{2.8}$$

This describes the nonlinear resonant interaction, and (2.8) are the kinematic conditions for the second-order resonance.

2.2 Resonance Conditions

A graphical procedure [5] to investigate the existence of solutions to the above underdetermined system (2.8) in 1D is given below. The following figures show the linear dispersion relations for gravity and gravity-capillary waves in water of infinite depth. In both cases, one chooses an arbitrary point (k_1, ω_1) and reproduces all branches of the linear dispersion relation with the origin translated to (k_1, ω_1) (in dashed lines on Figure 2.1). Let P be a point where the two curves intersect. Its coordinates in the original coordinate system are identified as (k_3, ω_3), and as (k_2, ω_2)

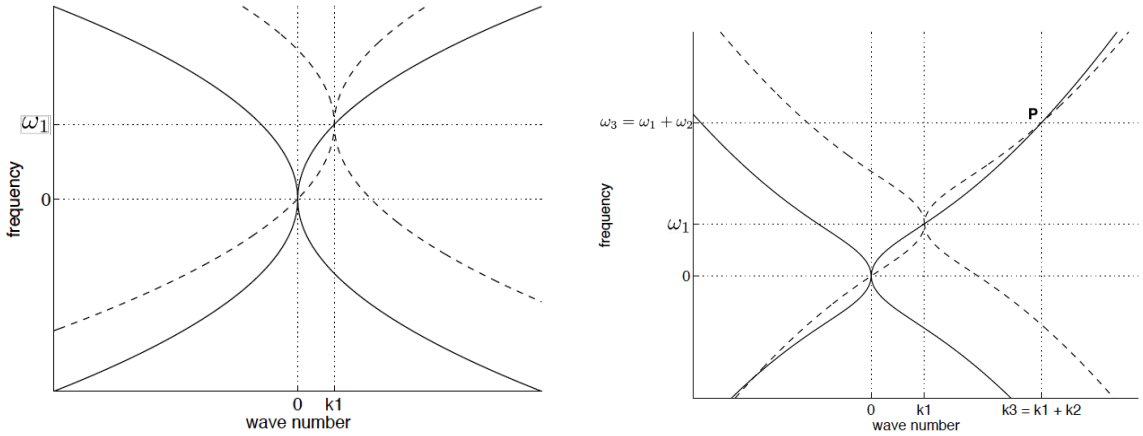

(a) (b)

Figure 2.1 Linear dispersion relation for gravity waves and gravity-capillary waves in water of infinite depth.

in the translated coordinate system. Then by construction, Equation (2.8) is satisfied. One can see on Figure 2.1 (a) that for gravity waves, the only such point is the origin, and therefore that the three-wave resonance does not exist. However, three-wave resonance is possible for gravity-capillary waves, as can be seen on Figure 2.1 (b).

2.3 The Water Wave Problem

The water wave problem describes the motion of an homogeneous, incompressible, irrotational fluid, whose free surface can be described as the graph of a function denoted $\zeta(\boldsymbol{x}, t)$. The spatial domain occupied by the fluid at time t is denoted $\Omega_t \subset \mathbb{R}^{d+1}$, $d = 1, 2$. The velocity of a particle located at $(\boldsymbol{x}, z) \in \Omega_t$ at time t, where $\boldsymbol{x}$ and z, respectively, denote the horizontal and vertical space variables is written $\boldsymbol{U}(\boldsymbol{x}, z, t) \in \mathbb{R}^{d+1}$. The assumed irrotationality also implies that there exists a velocity potential ϕ such that $\boldsymbol{U}(\boldsymbol{x}, z, t) = \nabla_{\boldsymbol{x},z}\phi$. In this setting, the free surface problem

can be written as

$$\begin{cases} \Delta_{\boldsymbol{x},z}\phi = 0 & \text{in } \Omega_t, \quad (2.9) \\ \partial_t\phi + \frac{1}{2}|\nabla_{\boldsymbol{x},z}\phi|^2 + \frac{p}{\rho} + gz = 0 & \text{in } \Omega_t, \quad (2.10) \\ \partial_t\zeta + \nabla_{\boldsymbol{x}}\phi \cdot \nabla_{\boldsymbol{x}}\zeta = \partial_z\phi & \text{on } z = \zeta(\boldsymbol{x},t), \quad (2.11) \\ \nabla_{\boldsymbol{x},z}\phi = 0 & \text{as } z \to -\infty. \quad (2.12) \end{cases}$$

To complete the problem, one can evaluate the Bernoulli equation at $z = \zeta$ to obtain

$$\partial_t\phi + \frac{1}{2}|\nabla_{\boldsymbol{x}}\phi|^2 - \frac{\gamma}{\rho}\nabla \cdot \left\{ \frac{\nabla_{\boldsymbol{x}}\zeta}{\sqrt{1+|\nabla_{\boldsymbol{x}}\zeta|^2)}} \right\} + g\zeta = 0, \quad (2.13)$$

where γ represent the surface tension, g is the acceleration of gravity, p is the pressure, and ρ is the fluid density.

2.4 The Pseudo-spectral Formulation

In his paper, Zakharov [29] made the remark that the knowledge of the free surface elevation ζ and the velocity potential evaluated at the free surface $\Phi = \phi|_{z=\zeta}$ fully defines the flow. Indeed, knowing $\Phi = \phi|_{z=\zeta}$ allows one to solve the following elliptic problem

$$\begin{cases} \Delta_{\boldsymbol{x},z}\phi = 0 & \text{in } \Omega_t, \quad (2.14) \\ \phi = \Phi & \text{on } z = \zeta(\boldsymbol{x},t), \quad (2.15) \\ \nabla_{\boldsymbol{x},z}\phi = 0 & \text{as } z \to -\infty. \quad (2.16) \end{cases}$$

Based on this fact, Choi [8] proposed a third-order asymptotic model for the weakly nonlinear evolution of gravity-capillary waves of small steepness. It is represented by a system of nonlinear PDEs for the surface displacement $\zeta(\boldsymbol{x},t)$ and the surface

velocity potential $\Phi(\boldsymbol{x}, t)$, which writes, under the second-order approximation, (after dropping the "$\boldsymbol{x}$" in the differential operators) as

$$\begin{cases} \partial_t \zeta + \mathcal{L}[\Phi] + \nabla\Phi \cdot \nabla\zeta + \zeta\Delta\Phi + \mathcal{L}[\zeta\mathcal{L}[\Phi]] = 0, \\ \partial_t \Phi + (g - \frac{\gamma}{\rho}\Delta)\zeta + \frac{1}{2}|\nabla\Phi|^2 - \frac{1}{2}(\mathcal{L}[\Phi])^2 = 0, \end{cases} \tag{2.17}$$

where $\mathcal{L}$ is the linear operator defined by

$$\mathcal{L}[f] = \int K(\boldsymbol{x} - \boldsymbol{\xi}) f(\boldsymbol{\xi}) \mathrm{d}\boldsymbol{\xi}, \qquad \mathcal{F}[K(\boldsymbol{x})] = -k, \quad \mathcal{L}[\mathrm{e}^{i\boldsymbol{k}\cdot\boldsymbol{x}}] = -k\mathrm{e}^{\mathrm{i}\boldsymbol{k}\cdot\boldsymbol{x}}, \tag{2.18}$$

with $\mathcal{F}$ representing the Fourier transform and $k = |\boldsymbol{k}|$. This is the formulation of the water waves problem for a single layer that will be used throughout this work.

CHAPTER 3

ONE-LAYER SYSTEM

3.1 Regions of Resonance

In this section, we examine the resonance conditions in order to investigate the resonance region in parameters space, where triad resonances are possible, and plot the variations of wavenumbers and frequencies within the region.

When $\boldsymbol{k}_j$ are written as

$$\boldsymbol{k}_j = k_j \left(\cos\theta_j, \sin\theta_j\right), \tag{3.1}$$

there are six unknowns (k_j and θ_j for j=1,2,3) among which three can be chosen in order to find numerical solutions to the resonance conditions given by Equation (2.8). After assuming $\theta_1 = 0$ without loss of generality, one can express k_j $(j = 1, 2, 3)$ in terms of θ_2 and θ_3. After nondimensionalizing k_j and ω_j as

$$K_j = (\sigma/g)^{1/2} k_j, \qquad \Omega_j = (\sigma/g^3)^{1/4} \omega_j, \tag{3.2}$$

the linear dispersion relations are given by

$$\Omega_j = K_j + K_j^3. \tag{3.3}$$

Then the resonance conditions given by (2.8) are re-written as

$$K_2 \cos\theta_2 + K_3 \cos\theta_3 = K_1, \qquad K_2 \sin\theta_2 + K_3 \sin\theta_3 = 0, \tag{3.4}$$

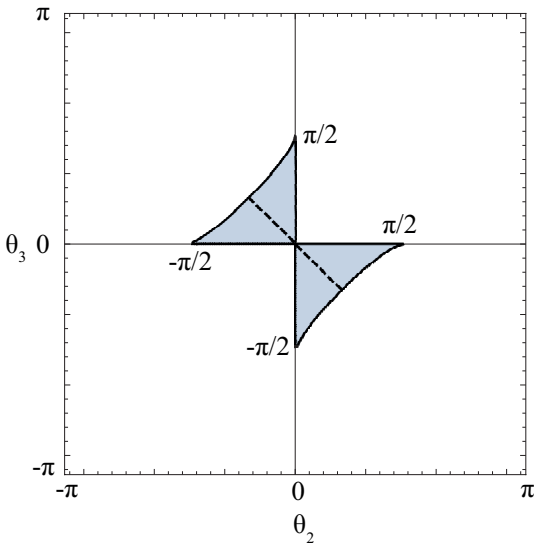

Figure 3.1 Region for resonant three-wave interactions (shaded area) in the (θ_2,θ_3)-plane defined by $f(\theta_1, \theta_2) > 0$, where f is defined by (3.10). The dashed line represents the symmetric case of $\theta_3 = -\theta_2$.

$$K_1^{1/2}\left(1+K_1^2\right)^{1/2} = K_2^{1/2}\left(1+K_2^2\right)^{1/2} + K_3^{1/2}\left(1+K_3^2\right)^{1/2}\ , \tag{3.5}$$

where $\Omega_j > 0$ have been assumed. Then K_2 and K_3 can be found as

$$K_2 = \frac{\sin\theta_3}{\sin\theta_{32}}K_1, \qquad K_3 = -\frac{\sin\theta_2}{\sin\theta_{32}}K_1, \tag{3.6}$$

where $\theta_{32} = \theta_3 - \theta_2$ vanishes only for one-dimensional waves, as can be seen from (3.4)-(3.5), which case will be discussed separately. When (3.6) is substituted into (3.5), an equation for K_1 can be obtained, in terms of θ_2 and θ_3, as

$$\left[\left(1+\frac{\sin^3\theta_2}{\sin^3\theta_{32}}-\frac{\sin^3\theta_3}{\sin^3\theta_{32}}\right)^2+4\frac{\sin^3\theta_2\sin^3\theta_3}{\sin^6\theta_{32}}\right]K_1^4$$

$$+2\left[\left(1+\frac{\sin\theta_2}{\sin\theta_{32}}-\frac{\sin\theta_3}{\sin\theta_{32}}\right)\left(1+\frac{\sin^3\theta_2}{\sin^3\theta_{32}}-\frac{\sin^3\theta_3}{\sin^3\theta_{32}}\right)\right.$$

$$+2\left(\frac{\sin^2\theta_2}{\sin^2\theta_{32}}+\frac{\sin^2\theta_3}{\sin^2\theta_{32}}\right)\frac{\sin\theta_2\sin\theta_3}{\sin^2\theta_{32}}\Bigg]K_1^2$$

$$+\left[\left(1+\frac{\sin\theta_2}{\sin\theta_{32}}-\frac{\sin\theta_3}{\sin\theta_{32}}\right)^2+4\frac{\sin\theta_2\sin\theta_3}{\sin^2\theta_{32}}\right]=0. \tag{3.7}$$

Before finding a region in the (θ_2,θ_3)-plane, where (3.7) has positive real roots for K_1^2, one should notice that, since K_2 and K_3 in (3.6) must be positive, the resonance region must be contained inside two triangular regions in the second and fourth quadrants of the (θ_2,θ_3)-plane, bounded by

$$\text{Region I:}\quad \theta_3=\theta_2+\pi,\qquad -\pi\le\theta_2\le 0,\qquad 0\le\theta_3\le\pi, \tag{3.8}$$

and

$$\text{Region II:}\quad \theta_3=\theta_2-\pi,\qquad 0\le\theta_2\le\pi,\qquad -\pi\le\theta_3\le 0. \tag{3.9}$$

As it can be confirmed numerically that the second and third coefficients of the quadratic equation for K_1^2 are negative inside Regions I and II while the discriminant is always positive there, (3.7) would have one positive root for K_1^2 along with one negative (or non-physical) root when the first coefficient is positive:

$$f(\theta_2,\theta_3)\equiv\left(\sin^3\theta_{32}+\sin^3\theta_2-\sin^3\theta_3\right)^2+4\sin^3\theta_2\sin^3\theta_3>\,0\,. \tag{3.10}$$

One more care must be taken as (3.7) is equivalent to $(\Omega_1^2-\Omega_2^2-\Omega_3^2)^2=(\pm2\Omega_2\Omega_3)^2$, as $K_1=K_2+K_3$ has been assumed. In other words, one should exclude a region where

$\omega_1 = \omega_2 - \omega_3$ instead of $\omega_1 = \omega_2 + \omega_3$. Figure 3.1 shows a region in the (θ_2, θ_3)-plane, in which a single positive solution of 3.7 for K_1 exists and, therefore, all resonant triads must lie. The boundary of this resonance region is given by $f(\theta_2, \theta_3) = 0$, which is tangent to the θ_2 and θ_3-axes at $\theta_2 = \pm\pi/2$ and $\theta_3 = \pm\pi/2$, respectively. Notice that the θ_2 and θ_3-axes should be excluded except for the origin (which corresponds to one-dimensional waves) since the resonance condition given by Equation (3.4) cannot be fulfilled if two waves are propagating in the x-direction while the third wave is propagating obliquely from the x-axis. While the resonant interaction of gravity-capillary waves has been investigated, no explicit region of resonance shown in Figure 3.1 has been previously given. Figures 3.2 and 3.3 show the variation of K_j and Ω_j inside the resonance region in the fourth quadrant of the (θ_2, θ_3)-plane. These plots allow to show, for a given value of, say, Ω_1, the possible range of the angles θ_2 and θ_3. Also, if a contour plot of the given value of Ω_1 is reproduced (in dashed line) on Figure 3.3(b), one can deduce the different associated triplets $(\Omega_2, \theta_2, \theta_3)$ that form a solution of the resonance conditions. The same fact can be stated for Ω_3 (Figure 3.3(c)).

Once the resonant conditions are satisfied, it is relevant and of interest to study the dynamic of the amplitudes of the three waves involved.

3.2 Dynamics: The Reduced Model for Waves Amplitudes

The complex wave amplitudes defined in Equation (2.6) satisfy a system of three ODEs. This is a generic, well known system describing three-wave resonant interaction. As a model for water waves triad resonance, it has been derived in different ways ([3], [25]), but we will here derive it from the second-order pseudo-spectral formulation described in Section 2.4. Inserting in (2.17) the expansions

$$\zeta = \epsilon\zeta^{(1)} + \epsilon^2\zeta^{(2)} + \dots . \qquad \Phi = \epsilon\Phi^{(1)} + \epsilon^2\Phi^{(2)} + \dots$$

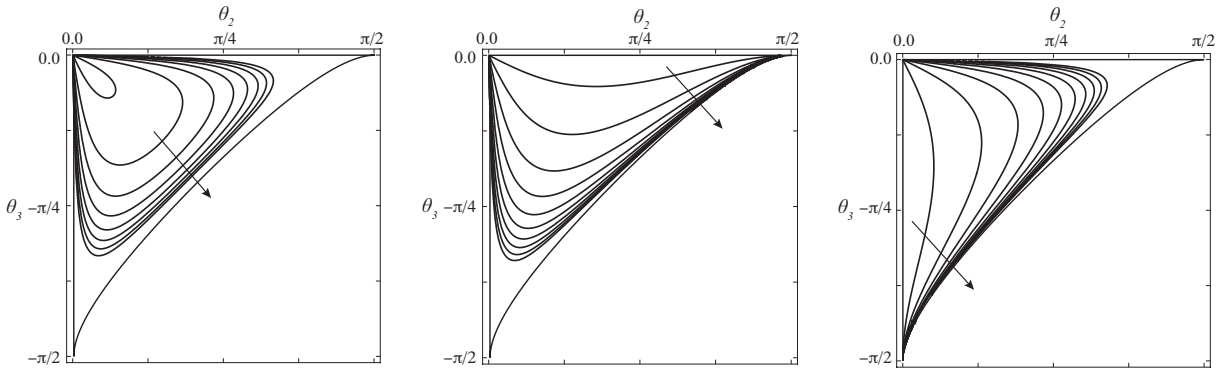

Figure 3.2 Contour plots of (dimensionless) resonant wavenumbers (K_j) in the fourth quadrant of the (θ_2, θ_3)-plane: (a) $3 < K_1 < 5$; (b) $0.5 < K_2 < 5$; (c) $0.5 < K_3 < 5$. The increment between the two neighboring contour levels is 0.5 and the arrows indicate the direction of increasing contour levels. Notice that the plot in (c) can be obtained from the plot in (b) by replacing θ_2 and θ_3 by $-\theta_3$ and $-\theta_2$, respectively, as there is no real distinction between θ_2 and θ_3.

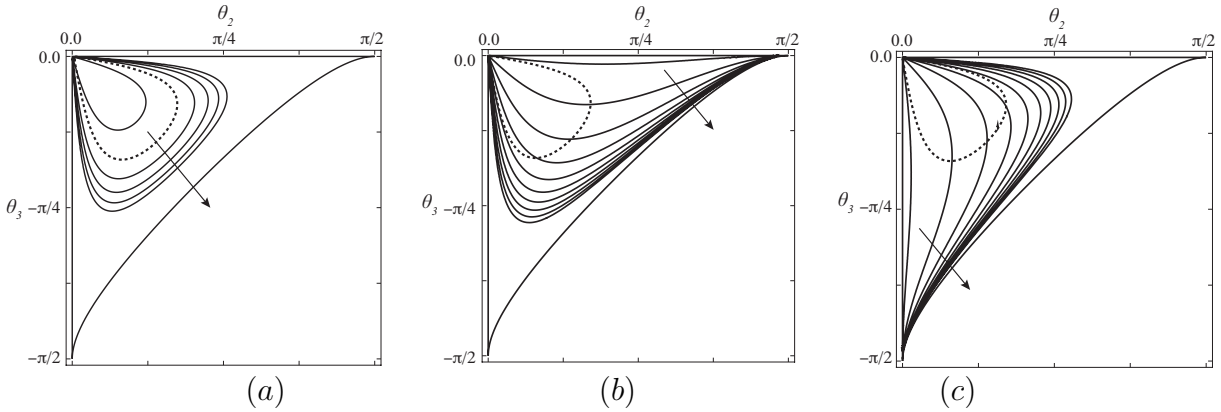

Figure 3.3 Contour plots of (dimensionless) resonant wave frequencies (Ω_j) in the fourth quadrant of the (θ_2, θ_3)-plane: (a) $2.5 \leq \Omega_1 \leq 5$; (b) $0.5 \leq \Omega_2 \leq 5$; (c) $0.5 \leq \Omega_3 \leq 5$. The increment between two neighboring contour levels is 0.5 and the arrows indicate the direction of increasing contour levels. To illustrate how to use these plots, as an example, the contour line of $\Omega_1 = 3$ is represented by a dashed curve in (a), which shows the relationship between θ_2 and θ_3 of all possible resonant triads with $\Omega_1 = 3$. Then, the values of Ω_2 and Ω_3 of the resonant triads with $\Omega_1 = 3$ can be determined by the levels of contour lines of Ω_2 and Ω_3 intersecting with the (dashed) contour line of $\Omega_1 = 3$, as shown in (b) and (c), respectively.

where $\epsilon \ll 1$ is the nonlinear parameter (wave slope) leads to the systems at the first and second order:

$$\mathcal{O}(\epsilon) \begin{cases} \partial_t \zeta^{(1)} + \mathcal{L}[\Phi^{(1)}] = 0, \\ \partial_t \Phi^{(1)} + (g - \frac{\gamma}{\rho}\Delta)\zeta^{(1)} = 0, \end{cases} \tag{3.11}$$

$$\mathcal{O}(\epsilon^2) \begin{cases} \partial_t \zeta^{(2)} + \mathcal{L}[\Phi^{(2)}] = -\nabla\Phi^{(1)} \cdot \nabla\zeta^{(1)} - \zeta^{(1)}\Delta\Phi^{(1)} - \mathcal{L}[\zeta^{(1)}\mathcal{L}[\Phi^{(1)}]], \\ \partial_t \Phi^{(2)} + (g - \frac{\gamma}{\rho}\Delta)\zeta^{(2)} = -\frac{1}{2}|\nabla\Phi^{(1)}|^2 + \frac{1}{2}(\mathcal{L}[\Phi^{(1)}])^2. \end{cases} \tag{3.12}$$

Since the goal is to capture three-wave interactions, we are looking for solutions of the form

$$\zeta^{(1)} = \sum_{j=1}^{3} a_j(t)\mathrm{e}^{\mathrm{i}\boldsymbol{k}_j\cdot\boldsymbol{x}}, \quad \Phi^{(1)} = \sum_{j=1}^{3} b_j(t)\mathrm{e}^{\mathrm{i}\boldsymbol{k}_j\cdot\boldsymbol{x}}. \tag{3.13}$$

Plugging these solutions into the first order equations gives

$$\begin{cases} \frac{da_j}{dt} - k_j b_j = 0 \\ \frac{db_j}{dt} + (g + \frac{\gamma}{\rho}k_j^2)a_j = 0 \end{cases} \qquad j = 1, 2, 3. \tag{3.14}$$

Looking for linear solutions $a_j = A_j\mathrm{e}^{-i\omega t}$, $b_j = B_j\mathrm{e}^{-i\omega t}$, we recover the well known linear dispersion relation for gravity-capillary wave in water of infinite depth:

$$\omega_j^2 = gk_j + \frac{\gamma}{\rho}k_j^3. \tag{3.15}$$

At the second order $\mathcal{O}(\epsilon^2)$, we know that the quadratic operator on the right-hand side will generate nonlinear interactions terms between different wave trains, and we also expect resonant terms on the right-hand side. Therefore, we introduce a slower timescale $\tau = \epsilon t$:

$$\zeta^{(1)} = \sum_{j=1}^{3} A_j(\tau) \mathrm{e}^{-\mathrm{i}\omega t} \mathrm{e}^{\mathrm{i}\boldsymbol{k}_j \cdot \boldsymbol{x}} + \text{c.c.}, \quad \Phi^{(1)} = \sum_{j=1}^{3} B_j(\tau) \mathrm{e}^{-\mathrm{i}\omega t} \mathrm{e}^{\mathrm{i}\boldsymbol{k}_j \cdot \boldsymbol{x}} + \text{c.c.} \tag{3.16}$$

From this we have that $\partial_t \to \partial_t + \epsilon \partial_\tau$, and the second order equations become

$$\begin{cases} \partial_t \zeta^{(2)} + \mathcal{L}[\Phi^{(2)}] = -\partial_\tau \zeta^{(1)} - \nabla \Phi^{(1)} \cdot \nabla \zeta^{(1)} - \zeta^{(1)} \Delta \Phi^{(1)} - \mathcal{L}[\zeta^{(1)} \mathcal{L}[\Phi^{(1)}]] \\ \partial_t \Phi^{(2)} + (g - \frac{\gamma}{\rho}\Delta)\zeta^{(2)} = -\partial_\tau \Phi^{(1)} - \frac{1}{2}|\nabla \Phi^{(1)}|^2 + \frac{1}{2}(\mathcal{L}[\Phi^{(1)}])^2. \end{cases} \tag{3.17}$$

After computing explicitly each term of the right hand side of (3.17) (see appendix A), we can regroup all terms proportional to $\mathrm{e}^{\mathrm{i}\boldsymbol{k}_j \cdot \boldsymbol{x}}$ and seek solutions of the form

$$\zeta^{(2)} = \sum_{j=1}^{3} C_j e^{-\mathrm{i}\omega_j t} \mathrm{e}^{\mathrm{i}\boldsymbol{k}_j \cdot \boldsymbol{x}}, \quad \Phi^{(2)} = \sum_{j=1}^{3} D_j e^{-\mathrm{i}\omega_j t} \mathrm{e}^{\mathrm{i}\boldsymbol{k}_j \cdot \boldsymbol{x}} \tag{3.18}$$

Plugging these solutions into our second order system and using $B_j = \frac{-\mathrm{i}\omega_j}{k_j} A_j$, we eliminate C_j and D_j to obtain a system of evolution equations for A_j by canceling the secular terms. This allows us to find that the amplitudes A_j satisfy the nonlinear system of ODEs

$$\frac{dA_1}{d\tau} = \mathrm{i}\Gamma_1 A_2 A_3, \quad \frac{dA_2}{d\tau} = \mathrm{i}\Gamma_2 A_1 A_3^*, \quad \frac{dA_3}{d\tau} = \mathrm{i}\Gamma_3 A_1 A_2^*, \tag{3.19}$$

where the coefficients Γ_j are found to be [6]

$$\Gamma_1 = \frac{1}{2}\left[\omega_1 k_1 + \omega_2 k_2 - \omega_3 k_3 + \frac{k_1}{\omega_1}\omega_2\omega_3 - \boldsymbol{k}_2 \cdot \boldsymbol{k}_3 \left(\frac{k_1\omega_2\omega_3}{\omega_1 k_2 k_3} + \frac{\omega_2}{k_2} - \frac{\omega_3}{k_3}\right)\right], \quad (3.20)$$

$$\Gamma_2 = \frac{1}{2}\left[\omega_1 k_1 + \omega_2 k_2 - \omega_3 k_3 + \frac{k_2}{\omega_2}\omega_1\omega_3 - \boldsymbol{k}_1 \cdot \boldsymbol{k}_3 \left(\frac{k_2\omega_1\omega_3}{\omega_2 k_1 k_3} + \frac{\omega_1}{k_1} - \frac{\omega_3}{k_3}\right)\right], \quad (3.21)$$

$$\Gamma_3 = \frac{-1}{2}\left[\omega_1 k_1 + \omega_2 k_2 - \omega_3 k_3 + \frac{k_3}{\omega_3}\omega_1\omega_2 + \boldsymbol{k}_1 \cdot \boldsymbol{k}_2 \left(\frac{k_3\omega_1\omega_2}{\omega_3 k_1 k_2} + \frac{\omega_1}{k_1} + \frac{\omega_2}{k_2}\right)\right]. \quad (3.22)$$

3.3 Energy Conservation

On physical grounds we expect that, since the effects of viscosity are neglected so far, the energy of the system must remain constant. The total energy of a monochromatic wave is the sum of the kinetic, potential, and surface tension energy. Given a velocity potential φ, let us first compute the kinetic energy per unit area:

$$E_k = \frac{\rho}{2}\int_{-\infty}^{0} |\nabla\varphi|^2 \mathrm{dz}.$$

Using the solutions of the linearized problem, where a is the real amplitude, we have that

$$\nabla\varphi = \begin{pmatrix} -\frac{a\omega k_x}{k}\mathrm{e}^{kz}\cos(\boldsymbol{k}\cdot\boldsymbol{x} - \omega t) \\ -\frac{a\omega k_y}{k}\mathrm{e}^{kz}\cos(\boldsymbol{k}\cdot\boldsymbol{x} - \omega t) \\ -a\omega\mathrm{e}^{kz}\sin(\boldsymbol{k}\cdot\boldsymbol{x} - \omega t) \end{pmatrix},$$

and therefore

$$|\nabla\varphi|^2 = a^2\omega^2 \mathrm{e}^{2kz},$$

which yields

$$E_k = \frac{\rho}{2}\int_{-\infty}^{0} a^2\omega^2 \mathrm{e}^{2kz}\mathrm{dz} = \frac{\rho a^2\omega^2}{4k}. \tag{3.23}$$

For the potential energy per unit area, we need to take the average over a wavelength, namely

$$E_p = \frac{\rho g}{\lambda_x\lambda_y}\int_0^{\lambda_x}\int_0^{\lambda_y}\int_0^{\zeta} z\mathrm{dxdydz} = \frac{\rho g}{2\lambda_x\lambda_y}\int_0^{\lambda_x}\int_0^{\lambda_y}\zeta^2\mathrm{dxdy} =$$

$$= \frac{\rho g}{2\lambda_x\lambda_y}\int_0^{\lambda_x}\int_0^{\lambda_y} a^2\cos^2(\boldsymbol{k}\cdot\boldsymbol{x}-\omega t)\mathrm{dxdy} = \frac{\rho g a^2}{4}.$$

Now, the potential energy per unit area due to the surface tension is obtained as

$$E_\gamma = \frac{\gamma}{\lambda_x\lambda_y}\int_0^{\lambda_x}\int_0^{\lambda_y}\sqrt{1+|\nabla\zeta|^2}\mathrm{dxdy} - \gamma.$$

We have that

$$\nabla\zeta = \begin{pmatrix} -k_x a\sin(\boldsymbol{k}\cdot\boldsymbol{x}-\omega t) \\ -k_y a\sin(\boldsymbol{k}\cdot\boldsymbol{x}-\omega t) \\ 0 \end{pmatrix} \tag{3.24}$$

and hence

$$|\nabla\zeta|^2 = a^2k^2\sin^2(\boldsymbol{k}\cdot\boldsymbol{x}-\omega t).$$

We can then write

$$\begin{aligned}
E_\gamma &= \frac{\gamma}{\lambda_x\lambda_y}\int_0^{\lambda_x}\int_0^{\lambda_y}\sqrt{1+|\nabla\zeta|^2}\mathrm{dxdy}-\gamma \\
&= \frac{\gamma}{\lambda_x\lambda_y}\int_0^{\lambda_x}\int_0^{\lambda_y}\sqrt{1+a^2k^2\sin^2(\boldsymbol{k}\cdot\boldsymbol{x}-\omega t)}\mathrm{dxdy}-\gamma \\
&\approx \frac{\gamma}{\lambda_x\lambda_y}\int_0^{\lambda_x}\int_0^{\lambda_y}\left(1+\frac{a^2k^2}{2}\sin^2(\boldsymbol{k}\cdot\boldsymbol{x}-\omega t)\right)\mathrm{dxdy}-\gamma \\
&= \frac{\gamma a^2k^2}{4}.
\end{aligned}$$

Therefore, we have

$$\begin{aligned}
E_k+E_p+E_\gamma &= \frac{\rho a^2\omega^2}{4k}+\frac{\rho g a^2}{4}+\frac{\gamma a^2k^2}{4} \\
&= \frac{\rho a^2\omega^2}{4k}+\frac{a^2}{4}(\rho g+\gamma k^2) \\
&= \frac{\rho a^2\omega^2}{4k}+\frac{\rho a^2}{4k}\left(gk+\frac{\gamma k^3}{\rho}\right) \\
&= \frac{\rho a^2\omega^2}{4k}+\frac{\rho a^2\omega^2}{4k} \\
&= \frac{\rho a^2\omega^2}{2k}.
\end{aligned}$$

Then the total energy for the j^{th} mode is $E_j = \frac{1}{2}\rho\frac{\omega_j^2}{k_j}|A_j|^2$. Going back to (3.19), we can deduce

$$\begin{cases} \frac{2}{\rho}\frac{dE_1}{d\tau} = \mathrm{i}\frac{\Gamma_1\omega_1^2}{k_1}(A_1^*A_2A_3 - A_1A_2^*A_3^*) & (3.25) \\ \frac{2}{\rho}\frac{dE_2}{d\tau} = \mathrm{i}\frac{\Gamma_2\omega_2^2}{k_2}(A_1A_2^*A_3^* - A_1^*A_2A_3) & (3.26) \\ \frac{2}{\rho}\frac{dE_3}{d\tau} = \mathrm{i}\frac{\Gamma_3\omega_3^2}{k_3}(A_1A_2^*A_3^* - A_1^*A_2A_3). & (3.27) \end{cases}$$

The total energy then varies according to

$$\frac{2}{\rho}\sum_{j=1}^{3}\frac{dE_j}{d\tau} = \mathrm{i}(\frac{\Gamma_1\omega_1^2}{k_1} - \frac{\Gamma_2\omega_2^2}{k_2} - \frac{\Gamma_3\omega_3^2}{k_3})(A_1^*A_2A_3 - A_1A_2^*A_3^*). \tag{3.28}$$

If $\frac{\Gamma_1\omega_1^2}{k_1} - \frac{\Gamma_2\omega_2^2}{k_2} - \frac{\Gamma_3\omega_3^2}{k_3} = 0$ then the energy is conserved. Numerically this term is of the order of the truncation error (10^{-16}). Although its manipulation is lengthy, it can be shown analytically that the right-hand side of (3.28) vanishes.

3.4 Exact Solutions

It is known that (3.19) can be explicitly solved in terms of Jacobian elliptic functions when written in real variables. Upon writing $A_j = |A_j|\mathrm{e}^{\mathrm{i}\varphi_j}$ and defining $\Delta = \varphi_1 - \varphi_2 - \varphi_3$, the reduced model may be rewritten as the following system of six real equations:

$$\frac{d|A_1|}{d\tau} = \Gamma_1|A_2||A_3|\sin(\Delta), \quad \frac{d|A_2|}{d\tau} = -\Gamma_2|A_1||A_3|\sin(\Delta), \quad \frac{d|A_3|}{d\tau} = -\Gamma_3|A_1||A_2|\sin(\Delta), \tag{3.29}$$

$$\frac{d\varphi_1}{d\tau} = \Gamma_1\frac{|A_2||A_3|}{|A_1|}\cos(\Delta), \quad \frac{d\varphi_2}{d\tau} = \Gamma_2\frac{|A_1||A_3|}{|A_2|}\cos(\Delta), \quad \frac{d\varphi_3}{d\tau} = \Gamma_3\frac{|A_1||A_2|}{|A_3|}\cos(\Delta). \tag{3.30}$$

Note that the last three may be recast into

$$\frac{d\Delta}{d\tau} = |A_1||A_2||A_3|\left(\frac{\Gamma_1}{|A_1|^2} - \frac{\Gamma_2}{|A_2|^2} - \frac{\Gamma_3}{|A_3|^2}\right)\cos(\Delta). \tag{3.31}$$

From (3.29) and (3.30), it is found that the following are invariant quantities known as the Manley-Rowe relations:

$$\mathcal{L}_{12} = \frac{|A_1|^2}{\Gamma_1} + \frac{|A_2|^2}{\Gamma_2}, \quad \mathcal{L}_{13} = \frac{|A_1|^2}{\Gamma_1} + \frac{|A_3|^2}{\Gamma_3}, \quad \mathcal{L}_{23} = \mathcal{L}_{12} - \mathcal{L}_{13}, \tag{3.32}$$

$$\mathcal{L}_{\Delta} = |A_1||A_2||A_3|\cos(\Delta). \tag{3.33}$$

We want now to decouple the equations. In order to do so, we will use (3.4) to eliminate $\sin(\Delta)$ in (3.29) and the other three to eliminate the amplitudes. Doing so leads to

$$\left(\frac{d|A_1|^2}{d\tau}\right)^2 = 4\Gamma_1^2\left[\frac{\Gamma_2\Gamma_3}{\Gamma_1^2}|A_1|^6 - \frac{\Gamma_2\Gamma_3}{\Gamma_1}\left(\mathcal{L}_{12}+\mathcal{L}_{13}\right)|A_1|^4 + \Gamma_2\Gamma_3\mathcal{L}_{12}\mathcal{L}_{13}|A_1|^2 - \mathcal{L}_{\Delta}^2\right], \tag{3.34}$$

$$\left(\frac{d|A_2|^2}{d\tau}\right)^2 = 4\Gamma_2^2\left[-\frac{\Gamma_1\Gamma_3}{\Gamma_2^2}|A_2|^6 + \frac{\Gamma_1\Gamma_3}{\Gamma_2}\left(\mathcal{L}_{12}+\mathcal{L}_{23}\right)|A_2|^4 - \Gamma_1\Gamma_3\mathcal{L}_{12}\mathcal{L}_{23}|A_2|^2 - \mathcal{L}_{\Delta}^2\right], \tag{3.35}$$

$$\left(\frac{d|A_3|^2}{d\tau}\right)^2 = 4\Gamma_3^2\left[-\frac{\Gamma_1\Gamma_2}{\Gamma_3^2}|A_3|^6 + \frac{\Gamma_1\Gamma_2}{\Gamma_3}\left(\mathcal{L}_{13}-\mathcal{L}_{23}\right)|A_3|^4 + \Gamma_1\Gamma_2\mathcal{L}_{13}\mathcal{L}_{23}|A_3|^2 - \mathcal{L}_{\Delta}^2\right]. \tag{3.36}$$

Equations (3.34)-(3.36) are of the form

$$\left(\frac{d|A_j|^2}{d\tau}\right)^2 = \Gamma_j^2 P_j^{(3)}(|A_j|^2),$$

where $P_j^{(3)}(X)$ is a third degree polynomial function. Assuming $P_j^{(3)}(|A_j|^2)$ possesses three real roots $|A_j|_c^2 \geq |A_j|_b^2 \geq |A_j|_a^2 \geq 0$, (3.34)-(3.36) can be written as

$$\left(\frac{d|A_1|^2}{d\tau}\right)^2 = \Gamma_1^2\left[\frac{\Gamma_2\Gamma_3}{\Gamma_1^2}(|A_1|^2-|A_1|_a^2)(|A_1|^2-|A_1|_b^2)(|A_1|^2-|A_1|_c^2)\right], \tag{3.37}$$

$$\left(\frac{d|A_2|^2}{d\tau}\right)^2 = \Gamma_2^2\left[-\frac{\Gamma_1\Gamma_3}{\Gamma_2^2}(|A_2|^2-|A_2|_a^2)(|A_2|^2-|A_2|_b^2)(|A_2|^2-|A_2|_c^2)\right], \tag{3.38}$$

$$\left(\frac{d|A_3|^2}{d\tau}\right)^2 = \Gamma_3^2\left[-\frac{\Gamma_1\Gamma_2}{\Gamma_3^2}(|A_3|^2-|A_3|_a^2)(|A_3|^2-|A_3|_b^2)(|A_3|^2-|A_3|_c^2)\right]. \tag{3.39}$$

If we define

$$X_j^2 = \frac{|A_j|^2-|A_j|_a^2}{|A_j|_b^2-|A_j|_a^2}, \qquad \eta_j^2 = \frac{|A_j|_b^2-|A_j|_a^2}{|A_j|_c^2-|A_j|_a^2}, \tag{3.40}$$

then we obtain the following set of ODEs for X_j

$$\left(\frac{dX_1}{d\tau}\right)^2 = \frac{\Gamma_2\Gamma_3}{4}(|A_1|_c^2-|A_1|_a^2)(1-X_1^2)(1-\eta_1^2X_1^2), \tag{3.41}$$

$$\left(\frac{dX_2}{d\tau}\right)^2 = -\frac{\Gamma_1\Gamma_3}{4}(|A_2|_c^2-|A_2|_a^2)(1-X_2^2)(1-\eta_2^2X_2^2), \tag{3.42}$$

$$\left(\frac{dX_3}{d\tau}\right)^2 = -\frac{\Gamma_1\Gamma_2}{4}(|A_3|_c^2-|A_3|_a^2)(1-X_3^2)(1-\eta_3^2X_3^2), \tag{3.43}$$

which can be solved by the sine Jacobian elliptic functions sn [1]. Going back to the original dependent variables $|A_j|^2$, the solutions are given by

$$|A_1|^2(\tau) = |A_1|_a^2 + \Upsilon_1 \mathrm{sn}^2[\Psi_1\tau, \eta_1], \tag{3.44}$$

$$|A_2|^2(\tau) = |A_2|_a^2 + \Upsilon_2 \mathrm{sn}^2[\Psi_2\tau, \eta_2], \tag{3.45}$$

$$|A_3|^2(\tau) = |A_3|_a^2 + \Upsilon_3 \mathrm{sn}^2[\Psi_3\tau, \eta_3], \tag{3.46}$$

where

$$\Upsilon_j = |A_j|_b^2 - |A_j|_a^2, \qquad \Psi_1 = \frac{1}{2}\sqrt{\Gamma_2\Gamma_3(|A_1|_c^2 - |A_1|^2|_a)},$$

$$\Psi_2 = \frac{1}{2}\sqrt{-\Gamma_1\Gamma_3(|A_2|_c^2 - |A_2|^2|_a)}, \qquad \Psi_3 = \frac{1}{2}\sqrt{-\Gamma_1\Gamma_2(|A_3|_c^2 - |A_3|^2|_a)}.$$

Examples of such solutions are shown in Figure 3.4. It is known that (3.44)-(3.46) are $\frac{2K(\eta_j)}{\Psi_j}-$periodic functions where K is the complete elliptic integral of the first kind. As it has been shown, the energy of a wave train is proportional to $|A_j|^2$. Therefore, a system in which each wave train has a contant energy is equivalent to the amplitude being time-independent. We investigate next under which conditions three steady amplitude waves can interact through nonlinear resonance.

[1] If $y(u) = \mathrm{sn}(u;k)$, then $\left(\frac{\mathrm{d}y}{\mathrm{d}u}\right)^2 = (1-y^2)(1-k^2y^2)$

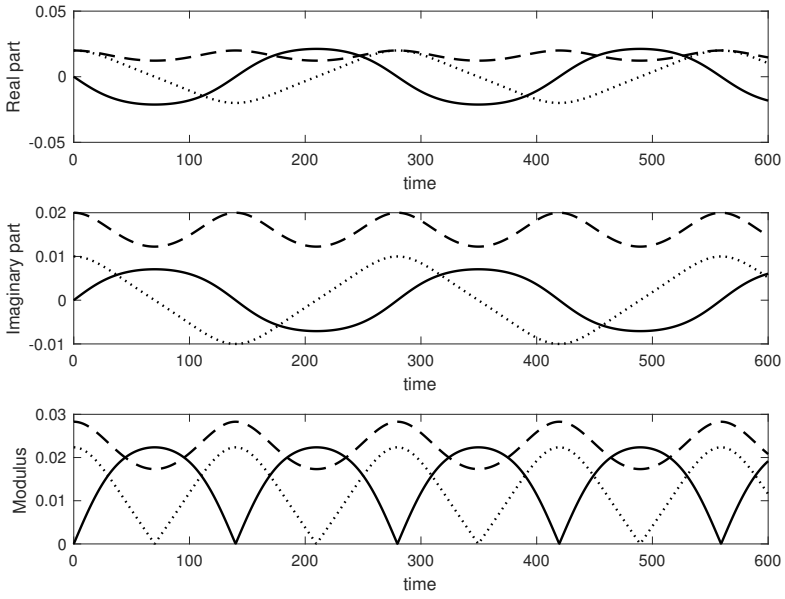

Figure 3.4 Numerical simulation of the resonant interactions of (from top to bottom): real part, imaginary part and modulus of A_1 (solid), A_2 (dashed) and A_3 (dotted). Here $\boldsymbol{k}_1 = [0, 1.8636]^T$, $\boldsymbol{k}_2 = [1.1899, 0.3681]^T$, $\boldsymbol{k}_3 = [0.6737, -0.3681]^T$ with initial conditions $A_1(0) = 0$, $A_2(0) = 0.01(1 + i)$ and $A_3(0) = 0.01(1 + 2i)$.

3.5 Resonant Interactions Without Energy Exchange

In general, there is an exchange of energy between the three waves constituting a resonant triad. However, for some particular initial conditions, the amplitudes will remain constant in time. Simmons [25] discussed possible triad solutions of constant amplitudes $|A_j|$ in addition to time-periodic and constant-phase (δ_j) solutions. Nevertheless no explicit conditions for the constant amplitude solutions were given. These steady state conditions correspond to the fixed points of (3.19) when expressed in real variables. For that reason, it is of interest to take a phase plane approach. We consider for simplicity, as well as for motivations which are presented in the next section, a symmetric configuration where $\theta_2 = -\theta_3$. Then the frequencies and wavenumbers are given in by

$$\Omega_1 = 2\Omega_2 = 2\Omega_3\,, \quad K_1 = 2\cos\theta_3\, K_2\,, \quad K_2 = K_3\,. \tag{3.47}$$

When the symmetric configuration is considered, (3.7) reduces to

$$\left(K_1^2 + 1\right)\left[\left(\cos^3\theta_3 - \tfrac{1}{2}\right) K_1^2 - (2 - \cos\theta_3)\cos^2\theta_3\right] = 0\,, \tag{3.48}$$

so that K_1 can be found as

$$K_1^2 = \frac{2(2 - \cos\theta_3)\cos^2\theta_3}{2\cos^3\theta_3 - 1} \qquad \text{for } -\theta_{\max} < \theta_3 < \theta_{\max}\,, \tag{3.49}$$

where the denominator must be positive so that the symmetric waves exist only when $|\theta_3| < \theta_{\max}$ with

$$\cos\theta_{\max} = 2^{-1/3}\,, \quad \text{or} \quad \theta_{\max} \simeq 37.467^o\,. \tag{3.50}$$

The same expression of the maximum angle was found by McGoldrick [19] from the resonance conditions for pure capillary waves. In order to plot the phase portraits of Equations (3.34)-(3.36), we consider the symmetry assumption, which simplifies the Manley-Rowe relations such that they are given by

$$\mathcal{L}_{12} = \mathcal{L}_{13} = \mathcal{L}, \qquad \mathcal{L}_{23} = 0. \tag{3.51}$$

Using (3.51) in (3.34)-(3.36) gives the dynamical system

$$\left(\frac{d|A_1|^2}{d\tau}\right)^2 = 4\Gamma_1^2\left(\frac{\Gamma_2^2}{\Gamma_1^2}|A_1|^6 - 2\frac{\Gamma_2^2}{\Gamma_1}\mathcal{L}|A_1|^4 + \Gamma_2^2\mathcal{L}^2|A_1|^2 - \mathcal{L}_\Delta^2\right) \tag{3.52}$$

$$\left(\frac{d|A_2|^2}{d\tau}\right)^2 = 4\Gamma_2^2\left(-\frac{\Gamma_1}{\Gamma_2}|A_2|^6 + \Gamma_1\mathcal{L}|A_2|^4 - \mathcal{L}_\Delta^2\right) \tag{3.53}$$

$$\left(\frac{d|A_3|^2}{d\tau}\right)^2 = 4\Gamma_3^2\left(-\frac{\Gamma_1}{\Gamma_3}|A_3|^6 + \Gamma_1\mathcal{L}|A_3|^4 - \mathcal{L}_\Delta^2\right), \tag{3.54}$$

It is convenient to simplify this system further by rescaling the coefficients Γ_j, (j=1,2,3) to unity. This procedure, described in appendix B, allow us to simplify the above dynamics system to

$$\left(\frac{d|A_1|^2}{dT}\right)^2 = 4\left(|A_1|^6 - 2\mathcal{L}|A_1|^4 + \mathcal{L}^2|A_1|^2 - \mathcal{L}_\Delta^2\right) \tag{3.55}$$

$$\left(\frac{d|A_2|^2}{dT}\right)^2 = 4\left(-|A_2|^6 + \mathcal{L}|A_2|^4 - \mathcal{L}_\Delta^2\right) \tag{3.56}$$

$$\left(\frac{d|A_3|^2}{dT}\right)^2 = 4\left(-|A_3|^6+\mathcal{L}|A_3|^4-\mathcal{L}_\Delta^2\right). \tag{3.57}$$

The right-hand sides of (3.55)-(3.57) can be regarded as third order polynomials in $|A_j|^2$. By looking at the discriminants of those polynomials, it is shown in appendix C that (3.55)-(3.57) hold under the parameter constraint $0 \leq \mathcal{L}_\Delta^2 \leq \frac{4}{27}\mathcal{L}^3$. After defining $\mathcal{X}_j = \mathcal{L}|A_j|^2$, $\tilde{T} = 4\mathcal{L}T$ and dropping the tilde, we show on Figure 3.5 the phase portraits of the dynamical system given by

$$\left(\frac{d\mathcal{X}_1}{dT}\right)^2 = \mathcal{X}_1^3 - 2\mathcal{X}_1^2 + \mathcal{X}_1 - \frac{\mathcal{L}_\Delta^2}{\mathcal{L}^3}, \tag{3.58}$$

$$\left(\frac{d\mathcal{X}_2}{dT}\right)^2 = -\mathcal{X}_2^3 + \mathcal{X}_2^2 - \frac{\mathcal{L}_\Delta^2}{\mathcal{L}^3}, \tag{3.59}$$

the equations for $|A_2|$ and $|A_3|$ being trivially identical. Figure 3.5 show that all solutions of (3.29) are stable, periodic functions. The outermost trajectories correspond to $\mathcal{L} = 0$. The fixed points correspond to $\mathcal{L}_\Delta^2 = \frac{4}{27}\mathcal{L}^3$ and are located at $\mathcal{X}_1 = \frac{1}{3}$ and $\mathcal{X}_2 = \frac{2}{3}$.

From an analytical point of view, one can see from (3.29)-(3.30) that $|A_j|$ are constant functions of time if

$$\varphi_1(0) - \varphi_2(0) - \varphi_3(0) = m\pi \quad \text{for } m{=}0{,}1\,, \tag{3.60}$$

$$\frac{\Gamma_1}{|A_1|^2} - \frac{\Gamma_2}{|A_2|^2} - \frac{\Gamma_3}{|A_3|^2} = 0 \quad \forall\tau. \tag{3.61}$$

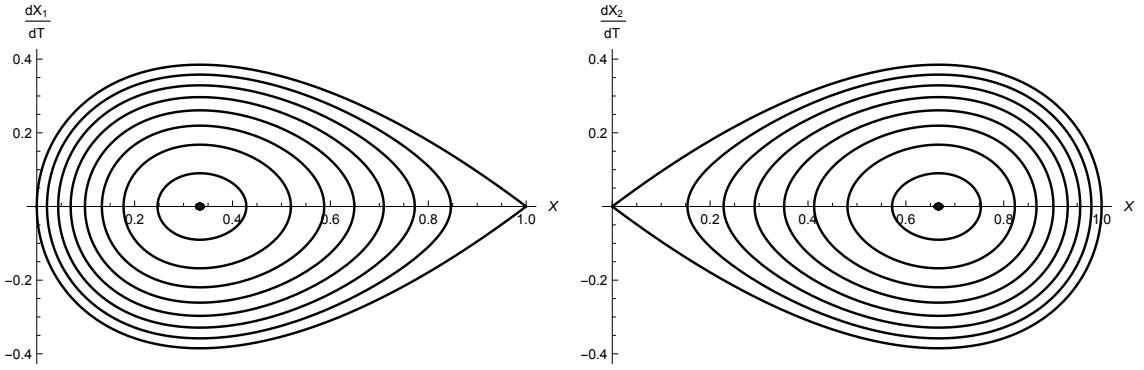

(a) **(b)**

Figure 3.5 Phase trajectories for the amplitudes (a) X_1 and (b) X_2. The outermost trajectories correspond to $\mathcal{L} = 0$. The fixed points correspond to $\mathcal{L}_\Delta^2 = \frac{4}{27}\mathcal{L}^3$ and are located at $X_1 = \frac{1}{3}$ and $X_2 = \frac{2}{3}$.

This is the no energy exchange conditions (NEEC). We also show that

$$\frac{\mathrm{d}\varphi_j}{\mathrm{d}\tau} = \Gamma_j \frac{|A_p||A_q|}{|A_j|} \cos\Delta\,, \tag{3.62}$$

with p and q being two remaining indices different from j. When the conditions for no energy exchange are met, φ_j can be found as

$$\varphi_j(\tau) = \mu_j\,\tau + \varphi_j(0)\,, \tag{3.63}$$

where μ_j representing the (constant) nonlinear frequency corrections are given by

$$\mu_j = (-1)^m\,\Gamma_j \frac{|A_p||A_q|}{|A_j|}\,. \tag{3.64}$$

Therefore when NEEC are met, we also have

$$\mu_1 - \mu_2 - \mu_3 = 0\,. \tag{3.65}$$

If the two conditions above are met along with the resonance conditions, the triad will interact through nonlinear resonance but without exchange of energy. The interaction will occur through the amplitude arguments φ_j. This implies that each wave is propagating in its own direction with a constant wave amplitude, but its wave speed is modified as a result of resonant interaction. This is obviously not the case in general, and moreover, this does in general not imply that the triad forms a traveling wave. As a simple example, the following system, valid for $\frac{\Gamma_1}{\Gamma_2+\Gamma_3} > 0$, is a resonant triad without exchange of energy:

$$\begin{cases} \mathrm{Im}[A_1] = 0, \quad \mathrm{Im}[A_2] = -\mathrm{Im}[A_3], \quad \mathrm{Re}[A_2] = \mathrm{Re}[A_3] \neq 0 \quad \text{(satisfies (4.19))} \\ \mathrm{Re}[A_1] = (\frac{\Gamma_1 |A_2|^2}{\Gamma_2+\Gamma_3})^{\frac{1}{2}} \quad \text{(satisfies (4.20))}. \end{cases}$$

Figure 3.6 show a numerical implementation of the above example. While the real and imaginary part remain periodic functions of time, the modulus of the amplitude, and therefore the energy, are time-independent. Steadiness of amplitudes is a necessary condition for resonant triad to form traveling waves. Along with that, the wave-trains must also all have the same total wave speed that is the sum of the linear wave speed and the nonlinear wave speed correction. This is the topic presented in the following section.

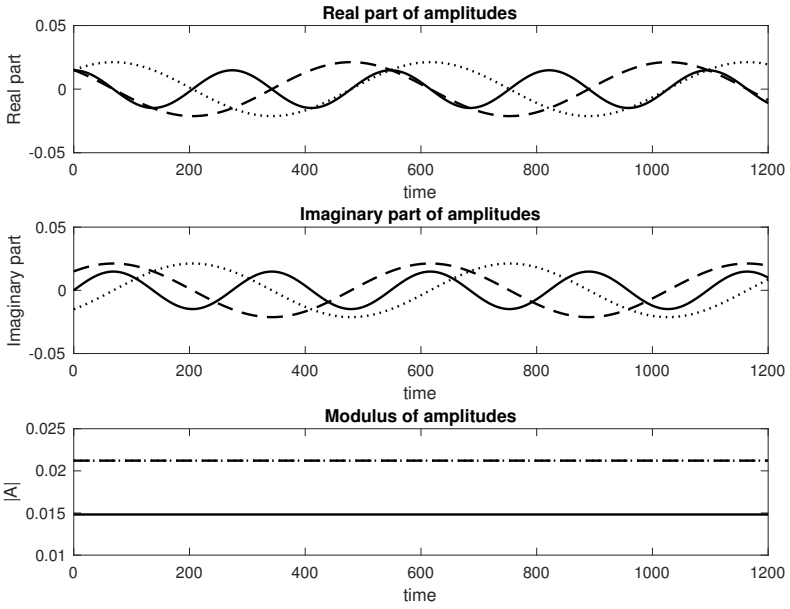

Figure 3.6 Numerical simulation of the resonant interactions with no exchange of energy between $|A_j|$, $j = 1, 2, 3$. Here $\boldsymbol{k}_1 = [0, 1.8636]^T$, $\boldsymbol{k}_2 = [1.1899, 0.3681]^T$, $\boldsymbol{k}_3 = [0.6737, -0.3681]^T$ with initial conditions $A_1 = 0.0096$, $A_2 = 0.01(1 + i)$ and $A_3(0) = 0.01(1 - i)$.

3.6 Traveling Wave Solutions

3.6.1 One-dimensional waves: Wilton ripples

It is known ([28], [21]) that a one-dimensional traveling wave field can be found for a resonant triad for $K_2 = K_3 = K_1/2 = 2^{-1/2}$. For this special case, the self-interaction of the K_2-wave excites the wave of wavenumber $2K_2$ at the second order, which is in turn in resonance with the K_1-wave. We derive here Wilton's traveling wave solution from the second order pseudo-spectral formulation. Writing $\theta = x - ct$ which implies $\partial_t \to -c\frac{d}{d\theta}$, $\partial_x \to \frac{d}{d\theta}$ in (2.17) gives (the primes standing for $\frac{d}{d\theta}$)

$$\begin{cases} -c\zeta' + \mathcal{L}[\Phi] + \Phi'\zeta' + \zeta\Phi'' + \mathcal{L}[\zeta\mathcal{L}[\Phi]] = 0 \\ -c\Phi' + (g - \frac{\gamma}{\rho}\frac{d^2}{d\theta^2})\zeta + \frac{1}{2}(\Phi')^2 - \frac{1}{2}(\mathcal{L}[\Phi])^2 = 0. \end{cases} \tag{3.66}$$

Plugging in 3.66 the Stokes expansion

$$\zeta = \epsilon\zeta_1 + \epsilon^2\zeta_2 + \dots, \quad \Phi = \epsilon\Phi_1 + \epsilon^2\Phi_2 + \dots, \quad c = c_0 + \epsilon c_1 + \epsilon^2 c_2 + \dots$$

leads to the systems:

$$\mathcal{O}(\epsilon) \begin{cases} -c_0\zeta_1' + \mathcal{L}[\Phi_1] = 0 \\ -c_0\Phi_1' + (g - \frac{\gamma}{\rho}\frac{d^2}{d\theta^2})\zeta_1 = 0, \end{cases}$$

$$\mathcal{O}(\epsilon^2) \begin{cases} -c_0\zeta_2' + \mathcal{L}[\Phi_2] = c_1\zeta_1' - \Phi_1'\zeta_1' - \zeta_1\Phi_1'' - \mathcal{L}[\zeta_1\mathcal{L}[\Phi_1]] \\ -c_0\Phi_2' + (g - \frac{\gamma}{\rho}\frac{d^2}{d\theta^2})\zeta_2 = c_1\Phi_1' - \frac{1}{2}(\Phi_1')^2 + \frac{1}{2}(\mathcal{L}[\Phi_1])^2. \end{cases}$$

Starting with the first order, we look for solutions of the form

$$\zeta_1 = a\mathrm{e}^{\mathrm{i}k\theta} + \text{c.c.}, \quad \Phi_1 = b\mathrm{e}^{\mathrm{i}k\theta} + \text{c.c.}.$$

This gives us the linear dispersion relation $c_0^2k^2 = gk + \frac{\gamma}{\rho}k^3$ and $a = \frac{ib}{c_0}$. At the second order we choose

$$\zeta_2 = p_1\mathrm{e}^{\mathrm{i}k\theta} + p_2\mathrm{e}^{2\mathrm{i}k\theta} + \text{c.c.}, \quad \Phi_2 = q_1\mathrm{e}^{\mathrm{i}k\theta} + q_2\mathrm{e}^{2\mathrm{i}k\theta} + \text{c.c.},$$

and obtain

$$\mathcal{O}(\epsilon^2)\begin{cases} -\mathrm{i}kc_0(p_1E + 2p_2E^2) - k(q_1E + 2q_2E^2) + \text{c.c.} = \mathrm{i}kc_1aE + \text{c.c.} + \dots \\ -\mathrm{i}kc_0(q_1E + 2q_2E^2) + (g + \frac{\gamma}{\rho}k^2)p_1E + (g + \frac{4\gamma}{\rho}k^2)p_2E^2 + \text{c.c} \\ = \mathrm{i}kc_1bE + k^2b^2E^2 + \text{c.c.} + \dots \end{cases}$$

where $E = \mathrm{e}^{\mathrm{i}k\theta}$, $E^2 = \mathrm{e}^{2\mathrm{i}k\theta}$. In that case, regrouping the coefficients of E, E^2 gives

$$\begin{cases} -\mathrm{i}kc_0p_1 - kq_1 = \mathrm{i}kc_1a \\ (g + \frac{\gamma}{\rho}k^2)p_1 - \mathrm{i}kc_0q_1 = kc_0c_1a \\ -2\mathrm{i}kc_0p_2 - 2kq_2 = 0 \\ (g + \frac{4\gamma}{\rho}k^2)p_2 - 2\mathrm{i}kc_0q_2 = -k^2c_0^2a^2. \end{cases}$$

The matrix for system for the variables (p_1, q_1) is singular. Moreover the solvability condition imposes that $c_1 = 0$. Solving the second order system gives the traveling wave solution

$$\zeta = 2\epsilon|a|\cos(k(x - c_0 t)) + \epsilon^2 2|p_2|\cos(2k(x - c_0 t)), \tag{3.67}$$

$$\Phi = 2c_0\epsilon|a|\cos(k(x - c_0 t)) + \epsilon^2 2|q_2|\cos(2k(x - c_0 t)), \tag{3.68}$$

where

$$p_2 = \frac{\mathrm{i}q_2}{c_0}, \quad q_2 = \frac{\mathrm{i}k^3 c_0^3 a^2}{(gk + \frac{4\gamma}{\rho}k^3) - 2k^2 c_0^2}. \tag{3.69}$$

There is a singularity in q_2 for some $k = k_w$ which actually corresponds to Wilton's ripples. In order to find this particular solution, we will expand the unknown as

$$\zeta = \epsilon(\zeta_1 + \tilde{\zeta_1}) + \epsilon^2\zeta_2 + \ldots, \quad \Phi = \epsilon(\Phi_1 + \tilde{\Phi}_1) + \epsilon^2\Phi_2 + \ldots, \quad c = c_0 + \epsilon c_1 + \epsilon^2 c_2 + \ldots \tag{3.70}$$

This now leads to:

$$\mathcal{O}(\epsilon) \begin{cases} -c_0(\zeta_1' + \tilde{\zeta}_1') + \mathcal{L}[\Phi_1 + \tilde{\Phi}_1] = 0 \\ -c_0(\Phi_1' + \tilde{\Phi}_1') + (g - \frac{\gamma}{\rho}\frac{d^2}{d\theta^2})(\zeta_1 + \tilde{\zeta}_1) = 0, \end{cases}$$

$$\mathcal{O}(\epsilon^2)\begin{cases} -c_0\zeta_2' + \mathcal{L}[\Phi_2] = c_1(\zeta_1' + \tilde{\zeta}_1') - (\zeta_1' + \tilde{\zeta}_1')(\Phi_1' + \tilde{\Phi}_1') - (\zeta_1 + \tilde{\zeta}_1)(\Phi_1'' + \tilde{\Phi}_1'') - \\ -\mathcal{L}[(\zeta_1 + \tilde{\zeta}_1)\mathcal{L}[(\Phi_1 + \tilde{\Phi}_1]] \\ \\ -c_0\Phi_2' + (g - \frac{\gamma}{\rho}\frac{d^2}{d\theta^2})\zeta_2 = c_1(\Phi_1' + \tilde{\Phi}_1') - \frac{1}{2}(\Phi_1' + \tilde{\Phi}_1')^2 + \frac{1}{2}(\mathcal{L}[\Phi_1 + \tilde{\Phi}_1])^2. \end{cases}$$

Starting with the first order, we look for solutions of the form

$$\zeta_1 = aE + \text{c.c.}, \quad \tilde{\zeta}_1 = \tilde{a}E^2 + \text{c.c.}, \quad \Phi_1 = bE + \text{c.c.}, \quad \tilde{\Phi}_1 = \tilde{b}E^2 + \text{c.c.}$$

This gives us the linear dispersion relation $c_0^2k^2 = gk + \frac{\gamma}{\rho}k^3$ and $a = \frac{\mathrm{i}b}{c_0}$ on one hand, and the relation $2k^2c_0^2 = gk + \frac{4\gamma}{\rho}k^3$ and $\tilde{a} = \frac{\mathrm{i}\tilde{b}}{c_0}$ on the other hand. At the second order and after plugging in the chosen ansatze in the right-hand side we choose

$$\zeta_2 = p_1E + p_2E^2 + c.c., \quad \Phi_2 = q_1E + q_2E^2 + c.c.,$$

which leads at the second order to the system

$$\mathcal{O}(\epsilon^2)\begin{cases} -\mathrm{i}kc_0(p_1E + 2p_2E^2) - k(q_1E + 2q_2E^2) + \text{c.c.} \\ = \mathrm{i}kc_1(aE + 2\tilde{a}E^2) - 2k^2\tilde{a}b^*E + \text{c.c.} + \dots \\ \\ -\mathrm{i}kc_0(q_1E + 2q_2E^2) + (g + \frac{\gamma}{\rho}k^2)p_1E + (g + \frac{4\gamma}{\rho}k^2)p_2E^2 + \text{c.c.} \\ = \mathrm{i}kc_1(bE + 2\tilde{b}E^2) + k^2b^2E^2 + \text{c.c.} + \dots \end{cases}$$

In that case, equating the coefficients of E, E^2 gives

$$\begin{cases} -\mathrm{i}kc_0p_1 - kq_1 = \mathrm{i}kc_1a - 2\mathrm{i}k^2c_0\tilde{a}a^* \\ (g + \frac{\gamma}{\rho}k^2)p_1 - \mathrm{i}kc_0q_1 = kc_0c_1a \\ -2\mathrm{i}kc_0p_2 - 2kq_2 = 2\mathrm{i}kc_1\tilde{a} \\ (g + \frac{4\gamma}{\rho}k^2)p_2 - 2\mathrm{i}kc_0q_2 = 2kc_0c_1\tilde{a} - k^2c_0^2a^2. \end{cases}$$

Here the matrices for both systems for the variables (p_1, q_1) and (p_2, q_2) are singular which gives two solvability conditions which impose that $\tilde{a} = \pm\frac{a^2}{2|a|}$ and $c_1 = \pm\frac{kc_0|a|}{2}$. This leads Wilton's ripples

$$\zeta = 2|a|\cos\psi + |a|\cos 2\psi, \tag{3.71}$$

where $\psi = k(x - c_0(1 \pm \epsilon\frac{k|a|}{2})t)$.

3.6.2 Two-dimensional Wilton ripples

We would like to propose a generalization to Wilton ripples for two-dimensional wave space. This means that, when the wave vectors of two propagating waves $\boldsymbol{k}_2 = [k, k_y]^T$ and $\boldsymbol{k}_3 = [k, -k_y]^T$ are aligned symmetrically about $\boldsymbol{k}_1 = [k_{1,x}, 0]^T$, their projection onto the x-axis verify $k_{1,x} = 2k$, as shown on Figure 3.7, and $\omega_1 = 2\omega$, where $\omega_1 = W(\boldsymbol{k}_1)$ and $\omega = W(\boldsymbol{k}_2)$. In this case, providing we choose A_1, A_2 and A_3 such that $|A_1|$ and $|A_2| = |A_3|$ remain constant for all time (which implies $\varphi_2 = \varphi_3$), we can show that the nonlinear wave speeds match and that, for well chosen initial conditions, the resulting surface elevation constitutes a traveling wave in the x-direction. In order to describe this, we first remark that the system of real ODEs (3.29-3.30) becomes, under the symmetry assumption,

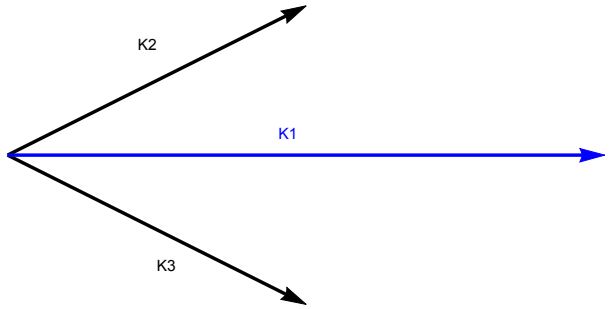

Figure 3.7 Symmetrical set-up.

$$\frac{d|A_1|}{d\tau} = \frac{i\omega}{2}\chi_1|A_2||A_3|\sin(\Delta), \quad \frac{d|A_2|}{d\tau} = \frac{i\omega}{2}\chi_2|A_1||A_3|\sin(\Delta), \quad \frac{d|A_3|}{d\tau} = \frac{i\omega}{2}\chi_3|A_1||A_2|\sin(\Delta), \tag{3.72}$$

$$\frac{d\varphi_1}{d\tau} = \frac{\omega}{2}\chi_1\frac{|A_2||A_3|}{|A_1|}\cos(\Delta) \quad \frac{d\varphi_2}{d\tau} = \frac{\omega}{2}\chi_2\frac{|A_1||A_3|}{|A_2|}\cos(\Delta) \quad \frac{d\varphi_3}{d\tau} = \frac{\omega}{2}\chi_3\frac{|A_1||A_2|}{|A_3|}\cos(\Delta), \tag{3.73}$$

where

$$\begin{cases} \chi_1 = 2k_2 - 3k + (k^2 - k_y^2)(\frac{2k_2+k}{k_2^2}) \\ \chi_2 = \chi_3 = 4k - 4k_2 + \frac{2k^2}{k_2}. \end{cases}$$

Hence, surface elevation ζ can be written as

$$\begin{aligned}
\zeta(t,\tau,\boldsymbol{u}) &= \sum_{j=1}^{3} A_j(\tau)\mathrm{e}^{\boldsymbol{k}_j\cdot\boldsymbol{x}-\omega_j t} + \text{c.c.} \\
&= 2|A_1|\cos(\boldsymbol{k}_1\cdot\boldsymbol{x}-\omega_1 t+\varphi_1) + 2|A_2|\cos(\boldsymbol{k}_2\cdot\boldsymbol{x}-\omega_2 t+\varphi_2) \\
&+ 2|A_3|\cos(\boldsymbol{k}_3\cdot\boldsymbol{x}-\omega_3 t+\varphi_3) \\
&= 2|A_1|\cos[2(kx-\omega t+\frac{\varphi_1}{2})] + 2|A_2|[\cos(kx-\omega t+\varphi_2+k_y y) \\
&+ \cos(kx-\omega t+\varphi_3-k_y y)] \\
&= 2|A_1|\cos[2(kx-\omega t+\frac{\varphi_1}{2})] + 4|A_2|\cos(kx-\omega t+\varphi_2)\cos(k_y y) \\
&= 2|A_1|\cos[2(kx-\omega(1\pm\frac{\chi_1}{2}\frac{|A_2|^2}{|A_1|}\epsilon)t] \\
&+ 4|A_2|\cos(kx-\omega(1\pm\frac{\chi_2}{2}|A_1|\epsilon)t)\cos(k_y y) \\
&= 2|A_1|\cos(2\psi_1) + 4|A_2|\cos(\psi_2)\cos(k_y y).
\end{aligned}$$

where

$$\psi_1 = kx-\omega\left(1\pm\frac{\chi_1}{2}\frac{|A_2|^2}{|A_1|}\epsilon\right)t, \quad \psi_2 = kx-\omega\left(1\pm\frac{\chi_2}{2}|A_1|\epsilon\right)t, \tag{3.74}$$

the + sign corresponding to $\Delta = 0$, and the − sign corresponding to $\Delta = \pi$. Finally,

$$\zeta = 2|A_1|(\tau)\cos(2\psi_1) + 4|A_2|(\tau)\cos(\psi_2)\cos(k_y y). \tag{3.75}$$

Therefore, (3.75) is traveling with a permanent periodic form in the x-direction if:

1. $|A_1|$ and $|A_2|$ are constant $\forall\tau$

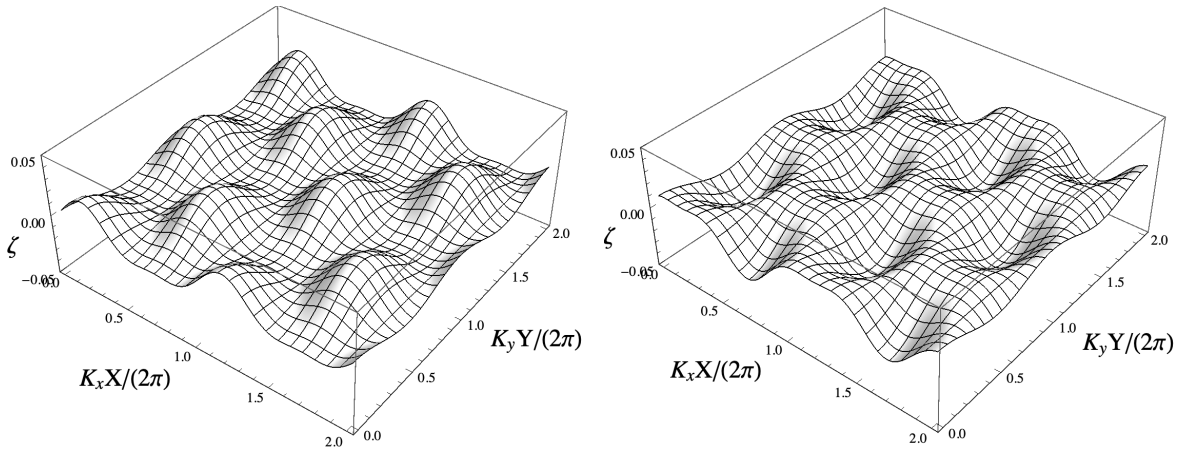

Figure 3.8 Symmetric Wilton ripples given by (73) with $K = 0.771$, $|A_2| = 0.004$, and $\theta = \theta_{\max}/3 = 12.489°$: (a) $m = 0$; (b) $m = 1$. In each plot, the surface wave field over two wave wave periods is shown.

2. $|A_2|^2 = \frac{\chi_2}{\chi_1}|A_1|^2$.

As one can see in Equation (3.74), each wave under this special resonance would propagate at a constant speed whose nonlinear correction to the linear wave speed is linearly proportional to wave steepness. This is more significant than Stokes' correction for monochromatic waves that is proportional to the square of wave steepness. To summarize, symmetry, along with the absence of energy exchange, imply the existence of traveling waves. Figure 3.8 shows an example of a two-dimensional Wilton ripples for dimensionless wavenumber $K = 0.771$, $|A_2| = 0.004$, $\theta = \theta_{\max}/3 = 12.489°$, and $\Delta = m\pi$ $(m = 0, 1)$.

Let us show that this 2D-Wilton ripples can also be recovered from the pseudo-spectral equations (2.17). If we define $\theta = x - ct$, then the second-order pseudo-spectral model becomes

$$\begin{cases} -c\partial_\theta\zeta + \mathcal{L}[\Phi] + \nabla\Phi\cdot\nabla\zeta + \zeta\Delta\Phi + \mathcal{L}[\zeta\mathcal{L}[\Phi]] = 0 & (3.76) \\ -c\partial_\theta\Phi + (g - \dfrac{\gamma}{\rho}\Delta)\zeta + \dfrac{1}{2}|\nabla\Phi|^2 - \dfrac{1}{2}(\mathcal{L}[\Phi])^2 = 0, & (3.77) \end{cases}$$

where $\nabla = [\partial_\theta, \partial_y]^T$. Plugging the expansions

$$\zeta = \epsilon(\zeta_1 + \tilde{\zeta_1}) + \epsilon^2\zeta_2 + \dots$$

$$\Phi = \epsilon(\Phi_1 + \tilde{\Phi}_1) + \epsilon^2\Phi_2 + \dots$$

$$c = c_0 + \epsilon c_1 + \epsilon^2 c_2 + \dots$$

leads to the systems:

$$\mathcal{O}(\epsilon)\begin{cases} -c_0\partial_\theta(\zeta_1 + \tilde{\zeta_1}) + \mathcal{L}[\Phi_1 + \tilde{\Phi}_1] = 0 \\ -c_0\partial_\theta(\Phi_1 + \tilde{\Phi}_1) + (g - \frac{\gamma}{\rho}\Delta)(\zeta_1 + \tilde{\zeta_1}) = 0, \end{cases}$$

$$\mathcal{O}(\epsilon^2)\begin{cases} -c_0\partial_\theta\zeta_2 + \mathcal{L}[\Phi_2] = c_1\partial_\theta(\zeta_1 + \tilde{\zeta_1}) - \nabla(\zeta_1 + \tilde{\zeta_1}) \cdot \nabla(\Phi_1 + \tilde{\Phi}_1) \\ \qquad\qquad -(\zeta_1 + \tilde{\zeta_1})\Delta(\Phi_1 + \tilde{\Phi}_1) - \mathcal{L}[(\zeta_1 + \tilde{\zeta_1})\mathcal{L}[\Phi_1 + \tilde{\Phi}_1]] \\ -c_0\partial_\theta\Phi_2 + (g - \frac{\gamma}{\rho}\Delta)\zeta_2 = c_1\partial_\theta(\Phi_1 + \tilde{\Phi}_1) - \frac{1}{2}|\nabla(\Phi_1 + \tilde{\Phi}_1)|^2 + \frac{1}{2}(\mathcal{L}[\Phi_1 + \tilde{\Phi}_1])^2. \end{cases}$$

Starting with the first order, we look for solutions of the form

$$\zeta_1 = a\cos(k_y y)E + c.c., \quad \tilde{\zeta_1} = \tilde{a}E^2 + c.c., \quad \Phi_1 = b\cos(k_y y)E + c.c., \quad \tilde{\Phi}_1 = \tilde{b}E^2 + c.c.$$

At the linear (first order) stage, this gives

$$\mathcal{O}(\epsilon)\begin{cases} -c_0 \mathrm{i}k(a\cos(k_y y)E + 2\tilde{a}E^2) - k_2 b\cos(k_y y)E - 2k\tilde{b}E^2 = 0 \\ -c_0 \mathrm{i}k(b\cos(k_y y)E + 2\tilde{b}E^2) + (g + \frac{\gamma}{\rho}k_2^2)a\cos(k_y y)E + (g + \frac{4\gamma}{\rho}k^2)\tilde{a}E^2 = 0, \end{cases}$$

which leads to the relations $a = \frac{\mathrm{i}k_2 b}{kc_0}$, $c_0^2 k^2 = gk_2 + \frac{\gamma}{\rho}k_2^3$, $\tilde{a} = \frac{\mathrm{i}\tilde{b}}{c_0}$ and $2k^2c_0^2 = gk + \frac{4\gamma}{\rho}k^3$. We obtain at the second order

$$\mathcal{O}(\epsilon^2)\begin{cases} -c_0\partial_\theta\zeta_2 + \mathcal{L}[\Phi_2] = [\mathrm{i}kc_1 a + (2k^2 - 2kk_2)a^*\tilde{b} - 2k^2\tilde{a}b^*]\cos(k_y y)E \\ \qquad\qquad + [2\mathrm{i}kc_1\tilde{a} + \frac{1}{2}(k^2 - k_y^2 + k_2(k_2 - 2k))ab]E^2 \\ -c_0\partial_\theta\Phi_2 + (g - \frac{\gamma}{\rho}\Delta)\zeta_2 = [\mathrm{i}kc_1 b + 2k(k_2 - k)b^*\tilde{b}]\cos(k_y y)E \\ \qquad\qquad + [2\mathrm{i}kc_1\tilde{b} + \frac{b^2}{4}(2k_2^2\cos(2k_y y) + k_2^2 + k^2 - k_y^2)]E^2, \end{cases}$$

which suggests the ansatze

$$\zeta_2 = p_1\cos(k_y y)E + (p_2 + p_3\cos(2k_y y))E^2, \quad \Phi_2 = q_1\cos(k_y y)E + (q_2 + q_3\cos(2k_y y))E^2.$$

Plugging those gives us the system for $\mathcal{O}(\epsilon^2)$

$$\begin{cases} -\mathrm{i}kc_0p_1 - k_2q_1 = \mathrm{i}kc_1a - \mathrm{i}c_0(2k^2 - 2kk_2)a^*\tilde{a} - \frac{2\mathrm{i}k^3c_0}{k_2}\tilde{a}a^* \\ (g + \frac{\gamma}{\rho}k_2^2)p_1 - \mathrm{i}kc_0q_1 = \frac{k^2c_0c_1}{k_2}a + \frac{2c_0^2k^2}{k_2}(k_2 - k)a^*\tilde{a} \\ -2\mathrm{i}kc_0(p_2 + p_3\cos(2k_yy)) - 2kq_2 - 2k_2q_3\cos(2k_yy) \\ \qquad = 2\mathrm{i}kc_1\tilde{a} - \mathrm{i}(2k^2 - 2kk_2)\frac{kc_0}{2k_2}a^2 \\ (g + \frac{4\gamma}{\rho}k^2)p_2 + (g + \frac{4\gamma}{\rho}k_2^2)p_3\cos(2k_yy) - 2\mathrm{i}kc_0(q_2 + q_3\cos(2k_yy)) \\ \qquad = 2kc_0c_1\tilde{a} - \frac{k^2c_0^2}{4k_2^2}(2k_2^2\cos(2k_yy) + 2k^2)a^2. \end{cases}$$

Here the solvability conditions write

$$c_1 = \frac{2c_0|a|^2\tilde{a}}{a^2}\left(k - k_2 + \frac{k^2}{2k_2}\right) \quad \text{and} \quad \tilde{a} = \frac{c_0a^2}{8c_1}\left(\frac{k^3}{k_2^2} + \frac{2k^2}{k_2} - 2k\right),$$

which gives

$$c_1 = \pm c_0|a|\sqrt{\frac{k}{8k_2^3}}(2kk_2 - 2k_2^2 + k^2), \qquad \tilde{a} = \pm\frac{a^2}{|a|}\sqrt{\frac{k}{8k_2}}.$$

The asymptotic solution then writes

$$\zeta = 2|a|\cos(k_yy)\cos(k(x - (c_0 + \epsilon c_1)t) + 2|\tilde{a}|\cos(2k(x - (c_0 + \epsilon c_1)t)).$$

CHAPTER 4

TWO-LAYER SYSTEM

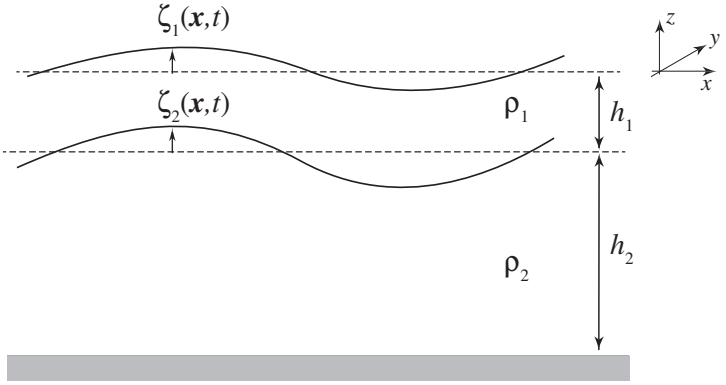

Figure 4.1 Two-layer system.

4.1 Resonance Conditions

We consider a two-layer system of inviscid fluid where ρ_j and h_j $(j = 1, 2)$ represent the fluid densities and thicknesses of the upper $(j = 1)$ and lower $(j = 2)$ layers, respectively (see Figure 4.1). Linear waves in this system satisfy the dispersion relations $\omega_\pm = W_\pm(k)$ between the wave frequency ω and the wavenumber k, where the positive and negative signs describe the surface and internal wave modes, respectively. In order to study this system, we rescale all physical quantities with respect to ρ_1, g, and h_1 so that the non-dimensionalized dispersion relations can be written as

$$\Omega_\pm^2 = \frac{K}{2(1 + TT_h/\rho)} \left[T + T_h \pm \sqrt{(T + T_h)^2 - 4TT_h(1 - 1/\rho)(1 + TT_h/\rho)} \right], \quad (4.1)$$

where $\omega_\pm^2 = (g/h_1)\Omega_\pm^2$, $K = h_1 k$, $\rho = \rho_2/\rho_1$ with $0 < 1/\rho < 1$ for stable stratification, $h = h_2/h_1$, $T = \tanh(K)$ and $T_h = \tanh(Kh)$. Note that the dispersion

relations have two physical parameters involved, namely ρ and h. In this system, three-wave resonant interactions occur when the wavenumbers $\boldsymbol{K}_j$ $(j = 1, 2, 3)$ and their associated positive wave frequencies Ω_j satisfy the conditions

$$\boldsymbol{K}_1 = \boldsymbol{K}_2 + \boldsymbol{K}_3\,, \qquad \Omega_1 = \Omega_2 + \Omega_3\,. \tag{4.2}$$

For one-dimensional waves, it has been known that there exists four classes of resonance, namely:

- class-I: interactions between two surface waves traveling in opposite directions and one internal wave [2]
- class-II: interactions between one surface wave and two internal waves traveling in opposite directions [14], [24]
- class-III: interactions between two surface waves traveling in the same direction and one internal wave [1]
- class-IV: interactions between one surface wave and two internal waves traveling in the same direction

To our knowledge, most of the studies focus on one-dimensional resonant wave interactions. We present in the next section a study of two-dimensional resonance conditions.

4.2 Two-dimensional Resonance

Given surface and internal modes, two types of triad resonances are possible. The first consists of two surface waves interacting with one internal wave, which will be referred to as type-A, and the other consists of one surface wave interacting with two internal waves, which will be called type-B.

4.2.1 Kinematic constraints for resonance

Using the polar form $\boldsymbol{K}_j = K_j(\cos\theta_j, \sin\theta_j)^T$ and assuming without loss of generality that the vector $\boldsymbol{K}_1$ is aligned with the x-axis, we have

$$K_1 = K_2\cos(\theta_2) + K_3\cos(\theta_3)\,, \qquad 0 = K_2\sin(\theta_2) + K_3\sin(\theta_3), \tag{4.3}$$

with $\theta_2 \in [0, \pi]$, $\theta_3 \in [\pi, 2\pi]$, which implies

$$\cos(\theta_2) = \frac{K_1^2 + K_2^2 - K_3^2}{2K_1K_2}, \qquad \cos(\theta_3) = \frac{K_1^2 + K_3^2 - K_2^2}{2K_1K_3}, \tag{4.4}$$

and given that $|\cos(\theta_j)| \leq 1$

$$(K_1 - K_2)^2 \leq K_3^2 \leq (K_1 + K_2)^2, \qquad (K_1 - K_3)^2 \leq K_2^2 \leq (K_1 + K_3)^2. \tag{4.5}$$

The equalities (4.4) hold for $\theta_{2,3} = 0, \pi$, which represent one-dimensional waves. Notice that the two equations in (4.5) are in fact equivalent and define a semi-infinite open tetrahedron T in the 3-dimensional space (K_2, K_3, K_1), and within which the first equation of (4.2) makes sense. Its lateral faces are defined by

$$K_1 = K_2 + K_3\,, \qquad K_1 = K_2 - K_3\,, \qquad K_1 = K_3 - K_2, \tag{4.6}$$

and constitute the geometrical constraints for 1-dimensional triad resonance. The second equation of (4.2) can be written in the form $F(K_1, K_2, K_3) = 0$, which is represented by a surface S in the (K_2, K_3, K_1)-space. Given a dispersion relation

W, triad resonance will therefore exist on the surface resulting from the intersection between S and T. Next, we are interested in finding the region in spectral space in which, for given physical parameters, the triad resonance between two-dimensional surface and internal gravity waves can occur.

4.2.2 Type-A resonance between two surface waves and one internal wave

We will assume in this section that $\boldsymbol{K}_1 = \boldsymbol{K}_1^+$ and $\boldsymbol{K}_2 = \boldsymbol{K}_2^+$ represent the wavenumber vectors of two surface waves while $\boldsymbol{K}_3 = \boldsymbol{K}_3^-$ is the wavenumber vector of the internal wave. It is also assumed that the wavenumbers satisfy the resonance condition $\Omega_1^+ = \Omega_2^+ + \Omega_3^-$. When the constraints described in §4.2.1 are met, we obtain a semi-infinite geometrical region referred to as the resonance region. Figure 4.2 (a) shows the intersection between the tetrahedron T and the surface S and 4.2 (b) the projection of this intersection in the (K_2^+, K_3^-)-space, which corresponds to the region for triad resonance of two surface and one internal waves. The edges (in short dashed lines) of the shaded region correspond to one-dimensional wave interactions. Indeed, the lower boundary is the projected intersection of the surface S with the plane $K_1^+ = K_2^+ + K_3^-$, and represents two surface and one internal waves all traveling in the same direction as can be seen from (4.3). This is known as class-III resonance and will be discussed later. The upper boundary on the other hand is the projection of S with the planw given by $K_1^+ = -K_2^+ + K_3^-$ and represents the so-called class-I resonance, where the two surface waves are counter propagative. The dot on the K_2^+-axis represents the critical wavenumber K_c^+ that satisfies the condition

$$d\Omega^+/dK|_{K=K_c^+} = \lim_{K\to 0} \Omega^-(K). \tag{4.7}$$

Class-III resonance occurs when at least one of the three wavenumbers is greater than K_c^+. This condition will be discussed in more details later. For the physical

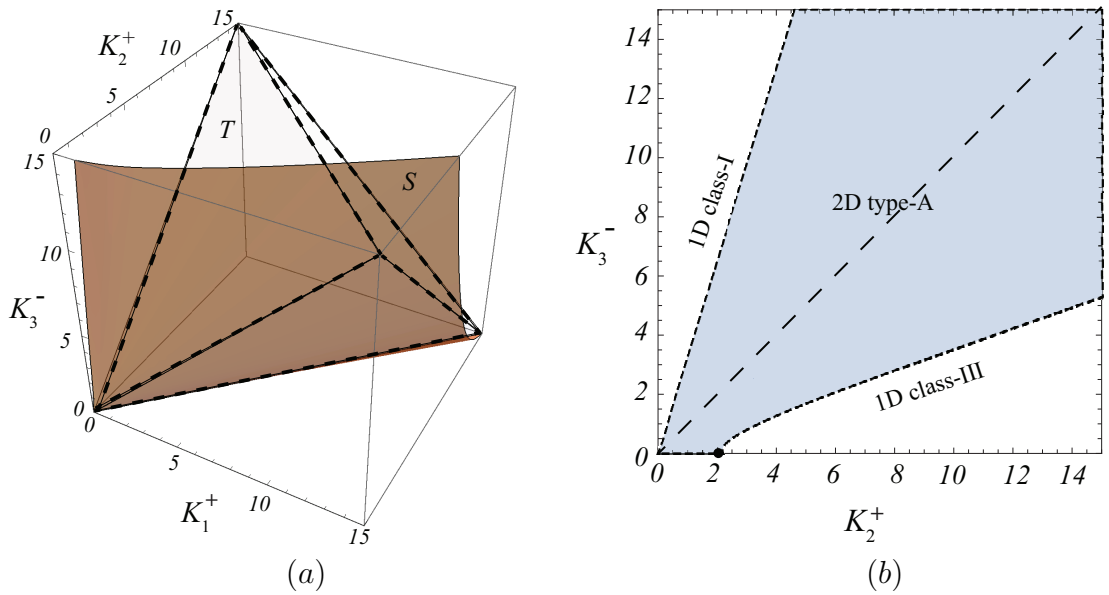

Figure 4.2 Type-A resonance for $\rho_2/\rho_1 = 1.163$ and $h_2/h_1 = 4$: (a) Surface S in the (K_1^+, K_2^+, K_3^-)-space. The dashed line represent the edges of the tetrahedron T; (b) Region of type-A resonance (shaded), which is the projection of S onto the (K_2^+, K_3^-)-plane. The boundaries (dashed) represent the 1D class-I and class-III resonant interactions. The black dot on the abscissa denotes the minimum wavenumber for the 1D class-III resonance: $K_{2m}^+ \approx 2.157$. The long dashed line represents the symmetric case of $K_2^+ = K_3^-$ and $\theta_2^+ = -\theta_3^-$.

parameters chosen in Figure 4.9, $K_c \approx 2.179$. Finally, The long dashed line represents symmetric interactions, where $K_2^+ = K_3^-$ and $\theta_2^+ = -\theta_3^-$.

4.2.3 Type-B: resonance between one surface wave and two internal waves

Here we assume that $\boldsymbol{K}_2 = \boldsymbol{K}_2^-$ and $\boldsymbol{K}_3 = \boldsymbol{K}_3^-$ represent internal waves and $\boldsymbol{K}_1 = \boldsymbol{K}_1^+$ the surface wave, and that they satisfy the resonance condition $\Omega_1^+ = \Omega_2^- + \Omega_3^-$. Figure 4.3 (a) shows the intersection between the semi-infinite open tetrahedron T and the surface S and 4.3 (b) the projection of this intersection in the (K_2^-, K_3^-)-space which corresponds to the region for triad resonance of on surface and two internal waves. The edges (in short dashed line) of the shaded region correspond to

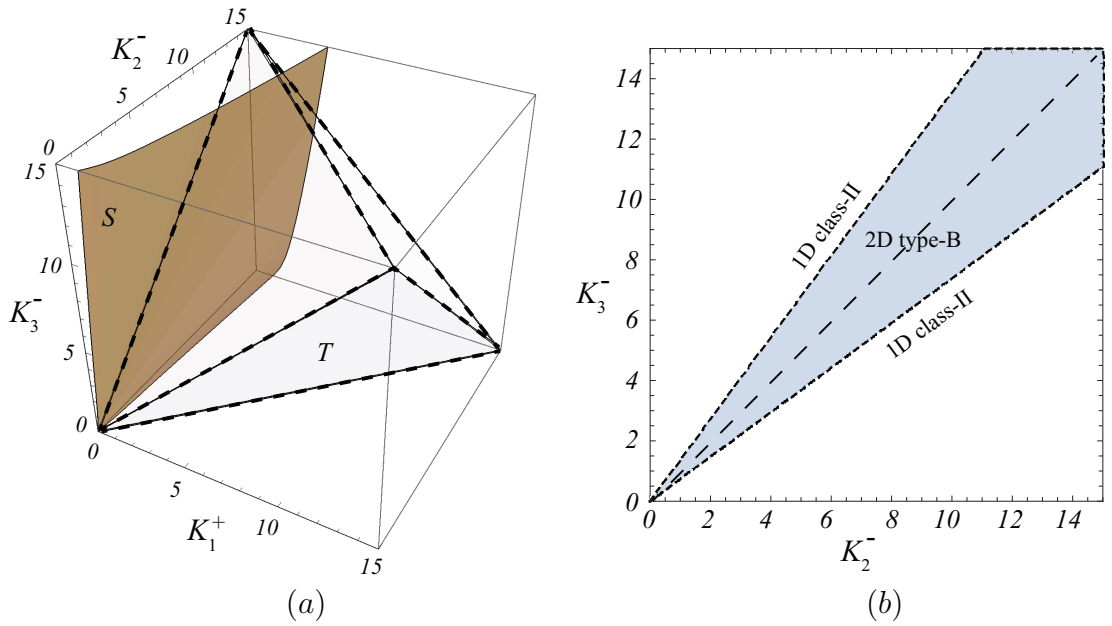

Figure 4.3 Type-B resonance for $\rho_2/\rho_1 = 1.163$ and $h_2/h_1 = 4$: (a) Surface S in the (K_1^+, K_2^-, K_3^-)-space. The dashed line represent the edges of the tetrahedron T; (b) Region of type-B resonance (shaded), which is the projection of S onto the (K_2^-, K_3^-)-plane. The boundaries (short-dashed) represent the 1D class-II resonant interactions. As the subscripts 2 and 3 and interchangeables, the region is symmetric along the long-dashed line which represents the symmetric Type-B resonance with $K_2^- = K_3^-$ and $\theta_2^- = -\theta_3^-$.

one-dimensional wave interactions. They are the projection of the intersections of S with the planes given by $K_1^+ = K_2^- + K_3^-$ and $K_1^+ = K_2^- - K_3^-$, respectively. The upper boundary corresponds to the surface wave traveling to the right while the lower boundary represents a left propagating surface wave. The long dashed line represents symmetric interactions.

To be discussed in the next section, for strong enough density ratio ($\rho > 3$), the resonance region for Type-B resonance changes qualitatively, and a fourth class of 1D-resonance emerges: the resonance region first widens, and is then split from infinity and is bounded by two outer and two inner boundaries. In this type of resonance (refers to as class-IV resonance), the three wave trains travel in the same direction. The existence of this class of one-directional triad resonance has been pointed out by Alam [1], but not presented explicitly. Figure 4.4 (a) shows the

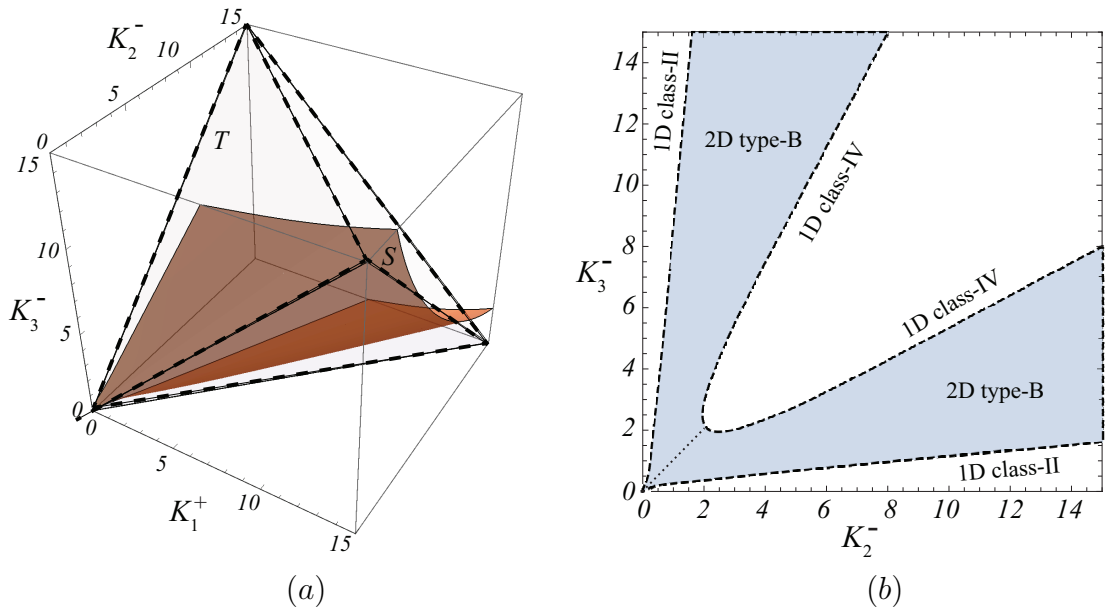

Figure 4.4 Type-B resonance for $\rho_2/\rho_1 = 3.1$ and $h_2/h_1 = 4$: (a) Surface S in the (K_1^+, K_2^-, K_3^-)-space. The dashed line represent the edges of the tetrahedron T; (b) Region of type-B resonance (shaded), which is the projection of S onto the (K_2^-, K_3^-)-plane. The boundaries (short-dashed) represent the 1D class-II and class-IV resonant interactions. The dotted line represents the symmetric type-B triad resonance.

intersection of tetrahedron T and the surface S for $\rho_2/\rho_1 = 3.1$ and $h_2/h_1 = 4$, while 4.4 (b) shows the spectral resonance region. The outer dashed boundaries of the resonance region represent as in the previous case class-II resonance, while the inner boundaries represent class-IV as the projection of T with the plane given by $K_1^+ = K_2^- + K_3^-$. The dotted line represents symmetric resonance.

One-dimensional waves are of interest as they can, under some circumstances, form traveling waves. First, the triad must consist of wave trains traveling in the same direction, from which class-I and class-II resonance should be excluded as potential physical settings for such solutions to be found. In what follows, we investigate in more details one-dimensional class-III and class-IV resonant interactions by finding the ranges of physical parameters in which they occur, as well as the conditions under which they can form traveling waves.

4.2.4 Co-propagating one-dimensional waves: class-III and class-IV resonant interactions

Recall that in the absence of the surface tension, non-dimensionalized dispersion relations for the system described above are given by

$$\Omega_{\pm}^2 = \frac{K}{2(1+\frac{TT_h}{\rho})}\left[T+T_h \pm \sqrt{(T+T_h)^2 - 4TT_h(1-\frac{1}{\rho})(1+\frac{TT_h}{\rho})}\right],$$

In the limiting case of $h_2 \to \infty$, we have

$$\Omega_+^2 = K, \qquad \Omega_-^2 = \frac{(1-\frac{1}{\rho})KT}{1+\frac{T}{\rho}}, \tag{4.8}$$

ρ being the only physical parameter. We will throughout this study make an extensive use of the group velocity $C_{g\pm} = d\Omega_{\pm}/dK$, whose behaviors are presented in the appendix. We now would like to find the set of physical parameters in which resonance is possible, as well as the existence and number of solutions of the resonance conditions within those regions. We will use subscripts S and I to distinguish surface and internal wave modes, while two waves belonging to the same mode will be identified by subscripts a and b. We will also use the following notations: $\Omega_{Si} = \Omega_+(K_{Si})$, $\Omega_{Ii} = \Omega_-(K_{Ii})$, $i = a, b$. Class-III resonance occurs when there exists K_{Sa}, K_{Sb} and K_I such that

$$|K_{Sa} - K_{Sb}| = K_I\,, \qquad |\Omega_{Sa} - \Omega_{Sb}| = \Omega_I. \tag{4.9}$$

As we will see next, (4.9) either has no solutions or two solutions. Graphically, (4.9) translates into finding an intersection between the branches of the internal mode dispersion relation whose origin has been translated to K_{Sa}, with the graph of the

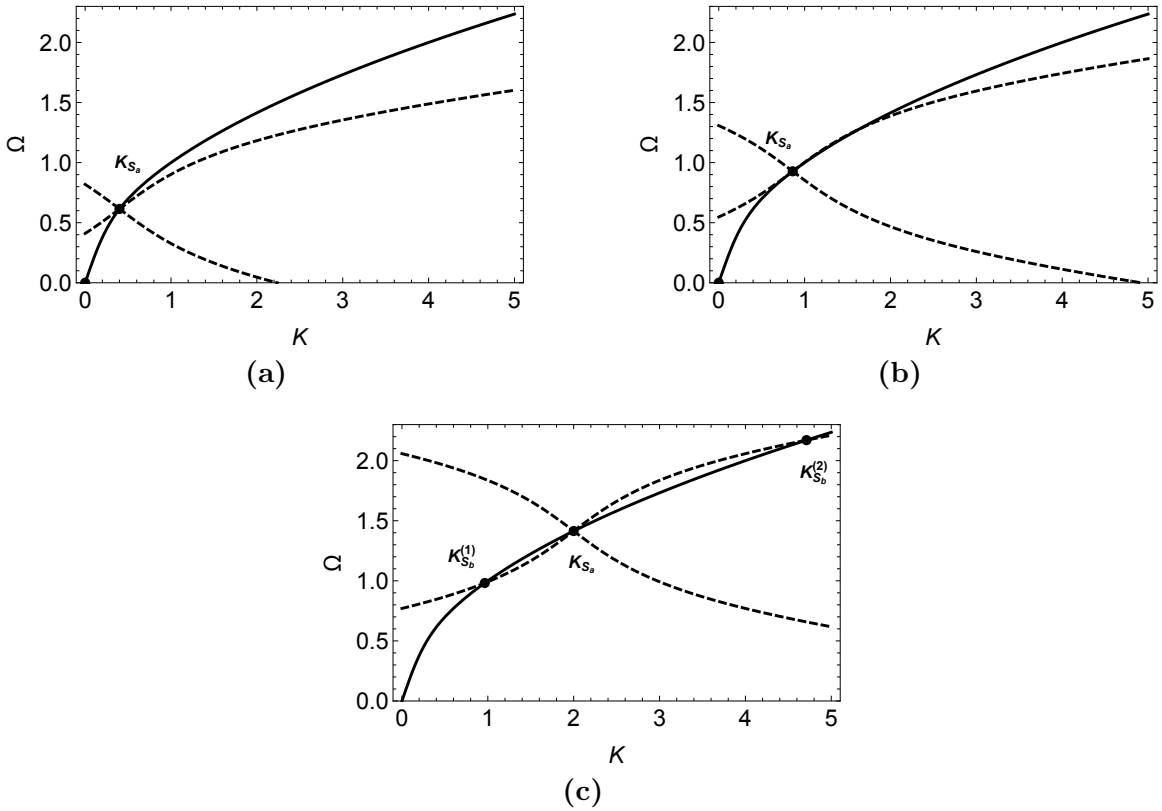

Figure 4.5 (a) Absence of class-III resonance (b) occurrence for critical wavenumber and (c) two different solutions for $\rho = 1/0.65$, $h = 3.7$.

surface mode dispersion relation. Since $\lim_{K\to 0} C_{g-}(K) = \sup_{K\in\mathbb{R}} C_{g-}$, one can see from Figure 4.5 that a necessary condition for class-III resonance is that the group velocity of the internal mode C_{g-} evaluated at the origin must be greater than the group velocity of the surface mode evaluated at the shifted origin. This condition formally writes

$$\lim_{K\to 0} C_{g-}(K) > C_{g+}(K_{Sa}). \tag{4.10}$$

The solution $K_{S_b}^{(1)}$ pictured in Figure 4.5 (c) is guaranteed by (4.10). The second solution pictured as $K_{S_b}^{(2)}$ is guaranteed by the fact that $\lim_{K\to\infty} C_{g-}(K)/C_{g+}(K) = [(1-1/\rho)/(1+1/\rho)]^{0.5} < 1$. Moreover, class-III resonance can occur for any value of the physical parameters $\rho > 1$ and $h \in (1,\infty)$. We will see in the next section that

taking surface tension into account restricts the admissible values of ρ and h. Figure 4.6 shows the critical wavenumber K^c_{Sa} as a function of $1/\rho$ for different values of h.

For strong enough density ratio, it is possible to obtain a fourth class of resonance

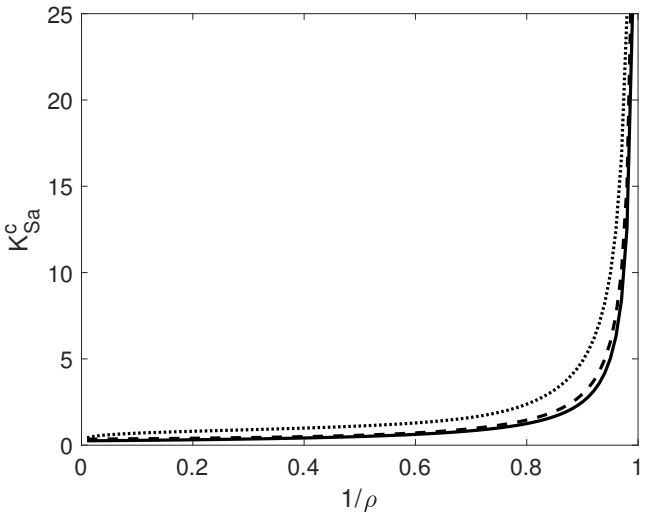

Figure 4.6 Critical wavenumber K^c_{Sa} as a function of $1/\rho$ for $h = 1$ (dotted), $h = 5$ (dashed) and $h \to \infty$ (solid).

that involves two internal waves traveling in the same direction along with one surface wave. A class-IV resonant triad satisfies

$$|K_{Ia}|+|K_{Ib}|= K_S\,, \qquad |\Omega_{Ia}|+|\Omega_{Ib}|= \Omega_S, \tag{4.11}$$

where K_{Ia} lies in the translated origin as shown in Figure 4.7. For short waves in infinite depth, the dispersion relation is given by (4.8), after taking the limit $K \to 0$, as

$$\Omega_+^2 = K, \qquad \Omega_-^2 = \frac{(1-\frac{1}{\rho})}{1+\frac{1}{\rho}}K. \tag{4.12}$$

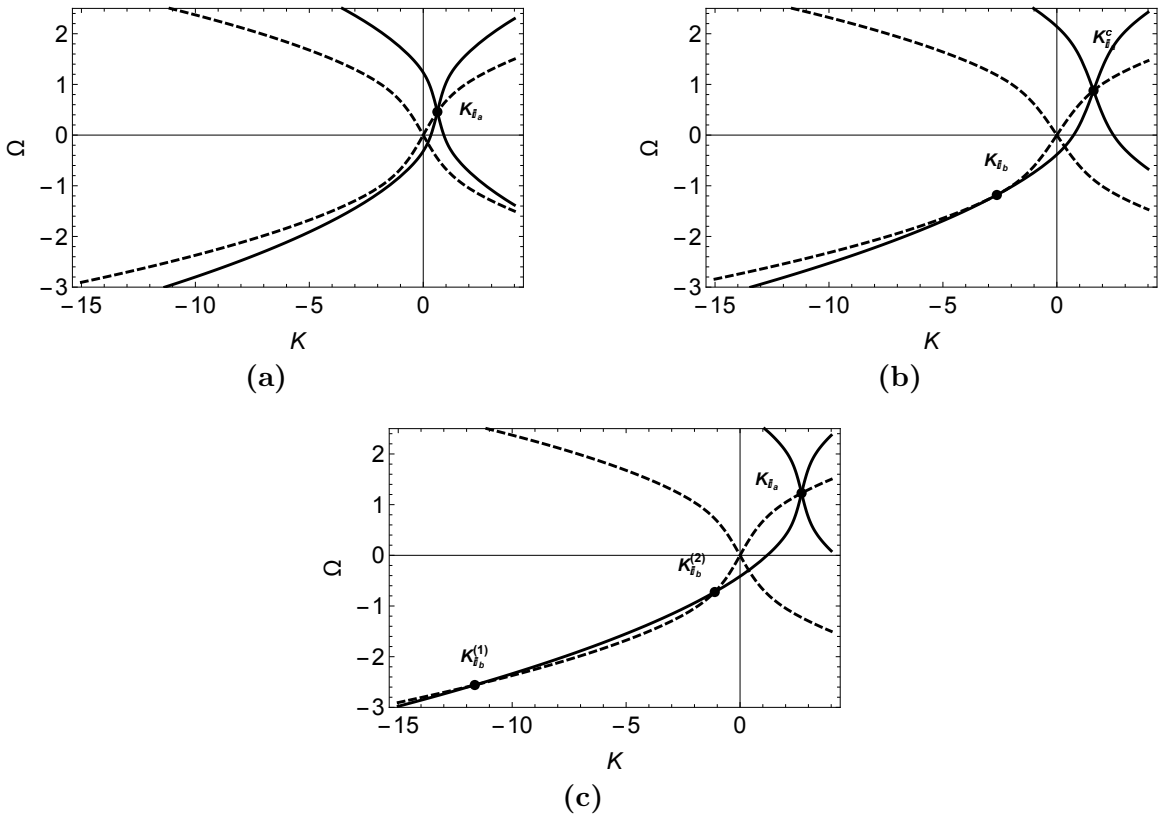

Figure 4.7 (*a*) Absence of class-IV resonance when $K_{Ia} < K_{Ia}^c$. (*b*) Occurrence for critical wavenumber $K_{Ia} = K_{Ia}^c$ and (*c*) two different solutions when $K_{Ia} > K_{Ia}^c$, in all three cases for $\rho = 1/0.3$.

The class-IV resonance conditions are then given by

$$K_1^+ = K_2^- + K_3^- \,, \qquad \sqrt{K_1^+} = \sqrt{\frac{\rho-1}{\rho+1}}\left(\sqrt{K_2^-} + \sqrt{K_3^-}\right), \tag{4.13}$$

which can be combined into

$$\left(\sqrt{K_2^-} - \sqrt{K_3^-}\right)^2 / \sqrt{K_2^- K_3^-} = \rho - 3 > 0. \tag{4.14}$$

Therefore, the 1D class-IV resonance occurs only for $\rho = \rho_2/\rho_1 > 3$. As all three waves are propagating in the same direction, the 1D class-IV resonance is similar to

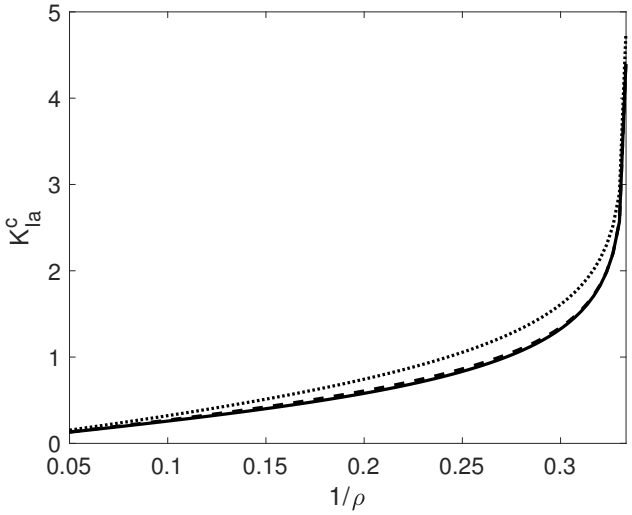

Figure 4.8 Critical wavenumber K^c_{Ia} as a function of $1/\rho$ for $h = 1$ (dotted), $h = 2$ (dashed) and $h \to \infty$ (solid).

the 1D class-III resonance although the latter is possible for any density ratio.

For fixed $\rho > 3$ there is some critical wavenumber K^c_{Ia} for which there is only one solution to the resonance conditions. One can see from Figure 4.7 (b) that the criticality condition writes

$$\Omega_-(K_{Ia}) + \Omega_-(K_{Ib}) = \Omega_+(K_{Ia} + K_{Ib}), \qquad C_{g+}(K_{Ia} + K_{Ib}) = C_{g-}(K_{Ib}).$$

Figure 4.8 shows the variations of the critical wavenumber K^c_{Ia} as a function of $1/\rho$ for different values of h.

4.3 Amplitude Equations

Dynamics of the resonance is described by a set of nonlinear evolution equations which has been derived by Choi [10] as a reduction model to the pseudo-spectral formulation proposed by Choi & Camassa [9] truncated at the second order in wave slope. It consists in the following system of three complex ODEs in which the symbols $\mathcal{F}_j$ (j=1,2,3) are used as generic functions and will later be replace by $\mathcal{A}_j$ for functions

of the surface wave mode and $\mathcal{B}_j$ for functions of the internal wave mode. The reduced model for triad interactions is

$$\frac{\mathrm{d}\mathcal{F}_1}{\mathrm{d}T} = \mathrm{i}\,\Gamma_1\,\mathcal{F}_2\mathcal{F}_3\,, \quad \frac{\mathrm{d}\mathcal{F}_2}{\mathrm{d}T} = \mathrm{i}\,\Gamma_2\,\mathcal{F}_3^*\mathcal{F}_1\,, \quad \frac{\mathrm{d}\mathcal{F}_3}{\mathrm{d}T} = \mathrm{i}\,\Gamma_3\,\mathcal{F}_1\mathcal{F}_2^*\,, \tag{4.15}$$

where Γ_j (j=1,2,3) are coefficients depending on wave-numbers and frequencies of each mode. The system (4.15) can be solved exactly in term of Jacobian elliptic functions as it has been shown in §3. The explicit amplitude equations specific to type-A and type-B resonance are derived in [10]. They can be obtained for type-A resonance as

$$\frac{\mathrm{d}\mathcal{A}_1}{\mathrm{d}T} = \mathrm{i}\,V^{(2)}_{1,2,3}\,\mathcal{A}_2\mathcal{B}_3\,, \quad \frac{\mathrm{d}\mathcal{A}_2}{\mathrm{d}T} = \mathrm{i}\,V^{(2)}_{1,2,3}\,\mathcal{A}_1\mathcal{B}_3^*\,, \quad \frac{\mathrm{d}\mathcal{B}_3}{\mathrm{d}T} = \mathrm{i}\,V^{(2)}_{1,2,3}\,\mathcal{A}_1\mathcal{A}_2^*\,, \tag{4.16}$$

and for type-B resonance as

$$\frac{\mathrm{d}\mathcal{A}_1}{\mathrm{d}T} = \mathrm{i}\,(V^{(5)}_{1,2,3} + V^{(5)}_{1,3,2})\,\mathcal{B}_2\mathcal{B}_3\,, \quad \frac{\mathrm{d}\mathcal{B}_{2,3}}{\mathrm{d}T} = \mathrm{i}\,(V^{(5)}_{1,2,3} + V^{(5)}_{1,3,2})\,\mathcal{A}_1\mathcal{B}_{2,3}^*\,, \tag{4.17}$$

where the coefficients $V^{(2)}_{1,2,3}$, $V^{(5)}_{1,2,3}$ and $V^{(5)}_{1,3,2}$ are given in the appendix E. Therefore, given a set of three wave modes (type-A or type-B), the solutions to (4.16)-(4.17) describe the time evolution of the complex amplitudes $\mathcal{A}_j$ and $\mathcal{B}_j$ that interact through triad resonant interaction of surface and internal waves. Given those solutions, one can reconstruct the expressions for the surface and internal elevations ζ_1 and ζ_2 that

are defined as

$$\zeta_1(\boldsymbol{x},t)=\sum_{j=1}^{3}a_+(\boldsymbol{k}_j,t)\mathrm{e}^{-\mathrm{i}\boldsymbol{k}_j\cdot\boldsymbol{x}}+\text{C.C.}\,,\qquad \zeta_2(\boldsymbol{x},t)=\sum_{j=1}^{3}a_-(\boldsymbol{k}_j,t)\mathrm{e}^{-\mathrm{i}\boldsymbol{k}_j\cdot\boldsymbol{x}}+\text{C.C.}\,, \tag{4.18}$$

where $\boldsymbol{a}=(a_+,a_-)^T\in\mathbb{C}^2$ is explicitly defined in Appendix F. The conditions for no energy exchange derived in Chapter 3 are generic to systems of ODEs like 4.15 that describe triad interactions. Therefore they describe one-layer as well as two-layer systems of waves. We recall that they write

$$\varphi_1(0)-\varphi_2(0)-\varphi_3(0)=m\pi \quad \text{for } m\text{=0,1,} \tag{4.19}$$

$$\frac{\Gamma_1}{|A_1|^2}-\frac{\Gamma_2}{|A_2|^2}-\frac{\Gamma_3}{|A_3|^2}=0 \quad \forall\tau. \tag{4.20}$$

In order for the triad to form a traveling wave, the wave-trains must have steady amplitudes and the same total wave speed. The latter condition is presented in the following section.

4.4 Traveling Waves

It is known that for a fluid with constant density, the only possible one-dimensional resonant triad to form a traveling wave is the so-called Wilton ripples. Indeed, when the surface tension is taken into account, the wave speed for one-layer gravity-capillary waves possesses a minimum, allowing two different wavenumbers to travel with the same wave speed. At the second order of nonlinearity, three modes satisfying $K_1=K_2+K_3$, $\Omega_1=\Omega_2+\Omega_3$ can travel with equal speed if $K_2=K_3$, namely when $K_1=2K_2$, $\Omega_1=2\Omega_2$. The latter system possesses a unique solution $K_2=2^{-1/2}$, for which a traveling wave solution known as Wilton ripples can be found.

As we mentioned earlier, in the two-layer system, traveling waves solutions are

to be sought for class-III and class-IV resonances, where a necessary condition is that all three modes involved travel with the same wave speed.

4.4.1 Conditions for traveling waves solutions

If steady wave trains possess equal linear wave speeds as well as equal nonlinear wave speed corrections, then they form a traveling wave. Wave speed functions for surface and internal modes, with and without surface tension, are presented in Figure 4.9 for some value of the physical parameters h_1, h_2 and ρ. One can see from Figure 4.9 (a) that without surface tension, three modes can possibly have the same wave speed only if there exists two internal modes and one surface mode such that $K_{Ia} = K_{Ib} = K_I$, namely $K_S = 2K_I$. This latter resonant triad, if it exists, falls into the fourth class of resonance. We will refer to this as a Wilton-type traveling wave solution, although modes of a different nature are involved. Once the NEEC is met, we can then expect to

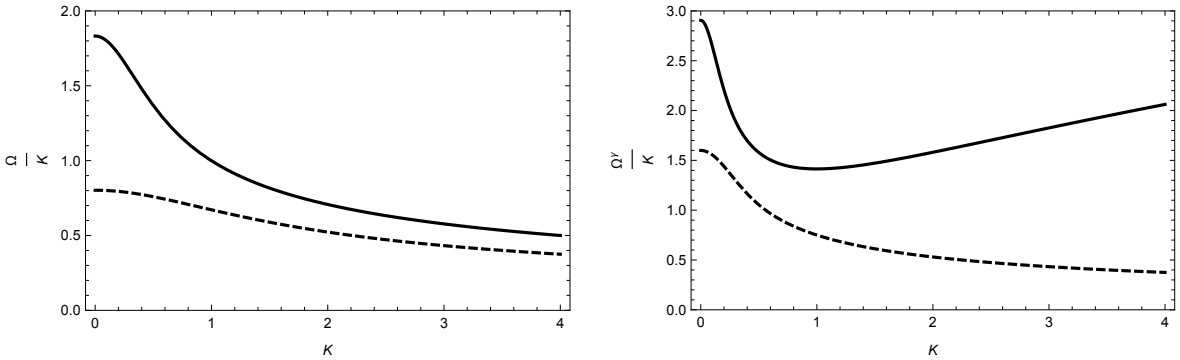

(a) (b)

Figure 4.9 Phase velocities of surface wave mode (solid) and internal wave mode (dashed) when (a) $\gamma_1 = 0$ and (b) $\gamma_1 \neq 0$.

find particular traveling wave solutions by separately matching the linear wave speeds and their nonlinear corrections. This is done in two steps: one with the kinematics of the problem (resonance conditions) and the other with the initial conditions. It is in fact sufficient to force the linear wave speeds to be equal. Indeed, it is always possible

to match the nonlinear corrections which in turn, implies the NEEC. Formally,

$$\begin{cases} K_1 = K_2 + K_3, \\ \frac{\Omega_1}{K_1} = \frac{\Omega_2}{K_2} = \frac{\Omega_3}{K_3}, \end{cases} \qquad \Rightarrow \qquad \Omega_1 = \Omega_2 + \Omega_3, \quad \text{(Resonance conditions)} \tag{4.21}$$

and

$$\begin{cases} K_1 = K_2 + K_3, \\ \frac{\mu_1}{K_1} = \frac{\mu_2}{K_2} = \frac{\mu_3}{K_3}, \end{cases} \qquad \Rightarrow \qquad \mu_1 = \mu_2 + \mu_3, \quad \text{(NEEC)} \tag{4.22}$$

assuming we impose $\Delta = m\pi$ $(m = 0, 1)$, as required by (4.19). Therefore, from (4.21)-(4.22) one can see that the set of traveling wave solutions constitutes a one-parameter family whose free parameter, once the wavenumbers have been fixed, can be arbitrarily chosen between μ_j $(j = 1, 2, 3)$, or equivalently $|A_j|$ $(j = 1, 2, 3)$.

4.4.2 Example

As mentioned before, when surface tension is not considered, a traveling wave formed by a resonant triad with matching linear wave speeds has to be of Wilton-type and belongs to the class-IV resonance. Such a traveling wave can be obtained if a numerical solution of

$$K_S = 2K_I, \qquad \Omega_S = 2\Omega_I \tag{4.23}$$

can be found after we choose appropriate initial conditions satisfying

$$|\mathcal{B}|^2 = 2|\mathcal{A}|^2. \tag{4.24}$$

Note that (4.23) implies that the equality of linear wave speed. A particular example of such a solution is given in Figure 4.11, where $K_I = 2.0716$, $K_S = 2K_I$, $\rho_2/\rho_1 = 3.1$, and $h_2/h_1 = 4$. In the case of finite depth, there are two physical parameters h and ρ. In this example, the wave slopes defined as $\varepsilon_S = K_S|a_+|/2\pi$ and $\varepsilon_I = K_I|a_-|/2\pi$ for the upper and internal surface, respectively, are $\varepsilon_S = 0.02$ and $\varepsilon_I = 0.01$. One can observe that the spacial period of the internal wave is twice as large as the one of the surface wave, which is what is expected for the class-IV resonance. In Figure 4.11 (a), the surface elevation ζ_1 seems to be a linear combination of two different modes. This is due to the fact that, as shown in Appendix F, the surface and interface elevations consist of the contributions from both internal and surface modes K_I and K_S. Figure 4.10 shows how the fundamental resonant wavenumber K_I, the solution of (4.23), behaves with respect to the density ratio ρ for different water depths.

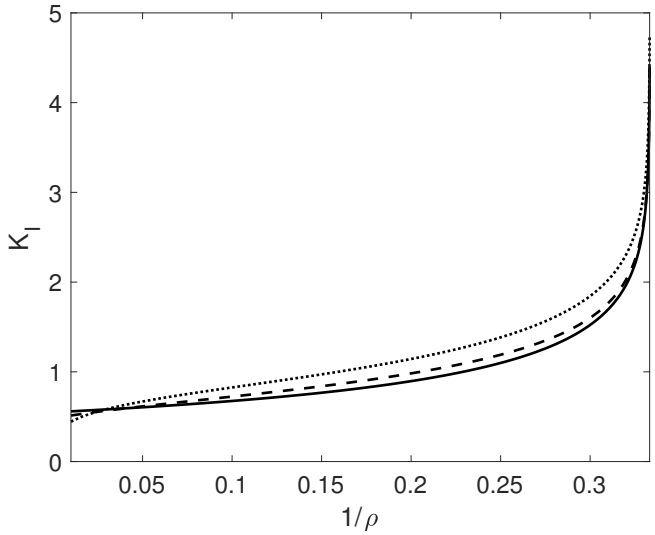

Figure 4.10 Traveling wave in class-IV without surface tension: variation of the fundamental wavenumber K_I with respect to the density ratio $1/\rho$ for $h = 1$ (dotted), $h = 1.5$ dashed and $h \to \infty$ (solid).

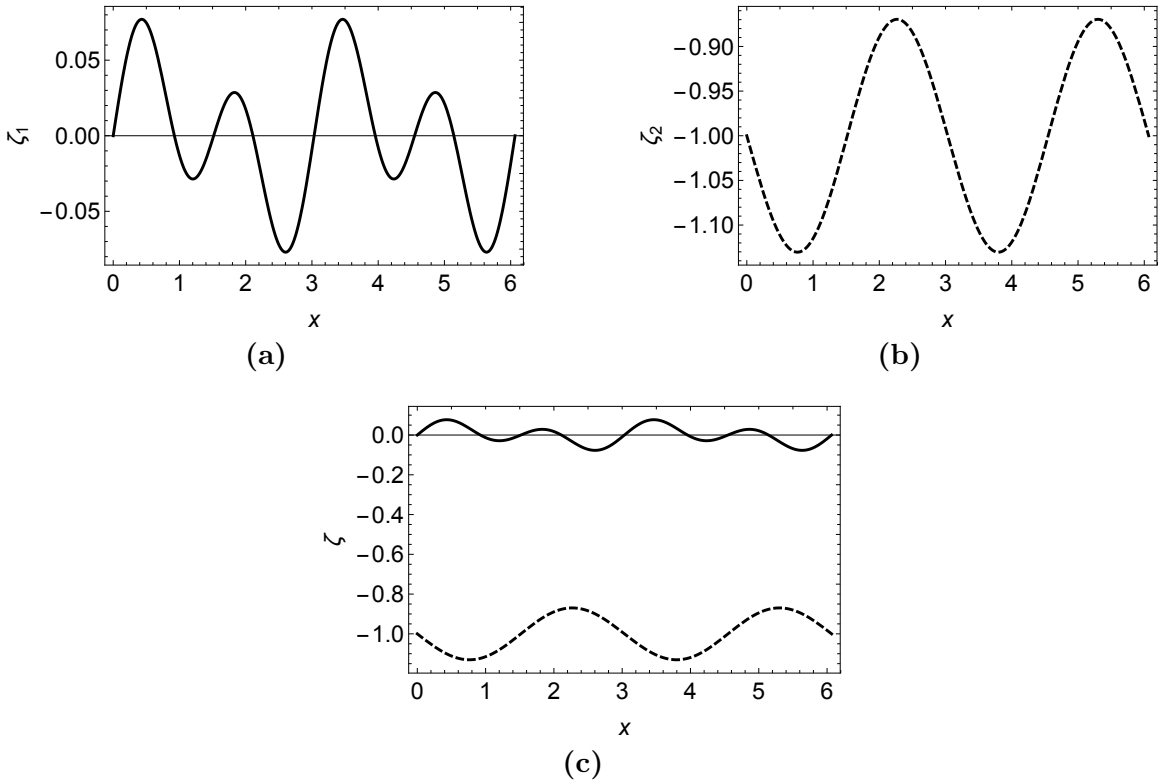

Figure 4.11 Surface elevation for traveling waves in class-IV resonance with $K_I = 2.0716$, $K_S = 2K_I$, $|Z_S| = 0.025$, $|Z_I| = 0.035$, $\rho_2/\rho_1 = 3.1$, $h_2/h_1 = 4$. (a) surface elevation ζ_1, (b) internal elevation ζ_2 and (c) both surface (solid) and internal (dashed) elevations.

4.5 Effects of Surface Tension

Taking into account surface tension implies the existence of a minimum for the surface mode wave speed, as shown in Figure 4.9 (b), which allows the possibility of three waves numbers satisfying $K_{Sb} - K_{Sa} = K_I$, and which would have the same linear wave speed. Hence, there might exist traveling waves under the class-III resonance. Note that the Wilton type traveling wave solution in class-IV would also be possible with surface tension. One could also see the necessity of surface tension for traveling waves in class-III from the dispersion relation graph: the wave speed being represented by the slope of a linear function intersecting the graph of $\Omega(K)$, the change of sign of the concavity of Ω induced by surface tension allows such a linear function to intersect the graph of the dispersion relation twice, which corresponds two different wavenumbers

traveling with equal wave speed.

In summary, in the absence of surface tension, the only possible traveling wave would satisfy class-IV resonance conditions, while the inclusion of surface tension provides another type of traveling wave that ultimately satisfies class-III resonant conditions.

4.5.1 Class-III resonance regions with surface tension

When only the surface tension on the top surface γ_1 is taken into account, the dispersion relation becomes

$$\begin{aligned}\Omega_{\pm}^2 =&\frac{K}{2(1+\frac{T_1T_h}{\rho})}\Bigg[T_1+T_h+K^2(T_1+\frac{T_h}{\rho}) \\ &\pm\sqrt{\left[T_1+T_h+K^2(T_1+\frac{T_h}{\rho})\right]^2-4T_1T_h(1-\frac{1}{\rho})(1+\frac{T_1T_h}{\rho})(1+K^2)}\Bigg],\end{aligned} \tag{4.25}$$

where we have nondimensionalized using

$$\omega_{\pm}^2=\frac{\rho_1 g^3}{\gamma_1}\Omega_{\pm}^2, \qquad k=\sqrt{\frac{\rho_1 g}{\gamma_1}}K, \qquad h_1=\sqrt{\frac{\gamma_1}{\rho_1 g}}H_1, \qquad h_2=h_1 h,$$

and where $\rho=\rho_2/\rho_1>1$, $T_1=\tanh(KH_1)$, $T_h=\tanh(KH_1h)$. Here three physical parameters are now involved, namely ρ, H_1 and h. Also, when $h\to\infty$, we have

$$\begin{aligned}\Omega_{\pm}^2 =&\frac{K}{2(1+\frac{T_1}{\rho})}\Bigg[T_1+1+K^2(T_1+\frac{1}{\rho}) \\ &\pm\sqrt{T_1^2(1+K^2)(\frac{2}{\rho}-1)^2+2T_1(1+K^2)(\frac{K^2}{\rho}+\frac{2}{\rho}-1)+(1+\frac{K^2}{\rho})^2}\Bigg].\end{aligned} \tag{4.26}$$

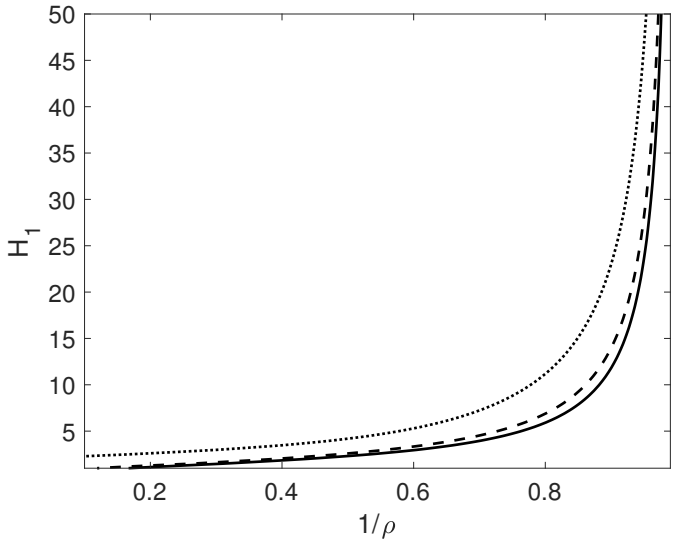

Figure 4.12 Class-III resonance parameter region in the (ρ, H_1)-space for for $h = 1$ (dotted), $h = 5$ (dashed) and $h \to \infty$ (solid). Resonance occurs in the region above the graph.

In the finite depth case, the group velocity of the surface wave has a finite limit when $K \to 0$, and is decreasing in a neighborhood of zero. As one can see on Figure 4.9 (b), a manifestation of the effect of γ_1 is that $\lim_{K\to\infty} C_{g+}(K) = \infty$, which implies the existence of a minimum for $C_{g+}(K)$. Therefore, in addition to the fact that the class-III resonance exists on a localized region of the physical parameters, the condition for the group velocity given by (4.10) is satisfied in an interval rather than on a semi-infinite subset of the wavenumbers. Moreover, within the parameter region, the condition $\lim_{K\to 0} C_{g-}(K) > \min_K C_{g+}(K)$ can only be met when $K_{Sa} \in (K^c_{Sa_1}, K^c_{Sa_2})$, where $K^c_{Sa_1}$ and $K^c_{Sa_2}$ are respectively the infimum and the supremum of the interval where (4.10) is satisfied.

In the case where $H_2 \to \infty$, using (4.26), we plot in Figure 4.13 the region of class-III resonance defined by the two critical wavenumbers K^c_{Sa1}, K^c_{Sa2} as functions of the physical parameters ρ and H_1. In the next section, we will look for specific resonant triads that form traveling waves, and present the conditions for their existence for the class-III resonance.

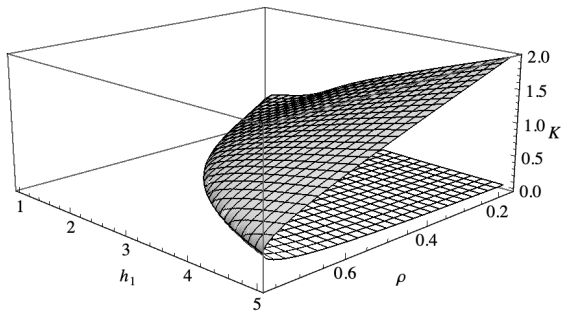

Figure 4.13 Class-III resonance region in the (ρ, H_1, K)-space when $H_2 \to \infty$. The lower surface corresponds to $K^c_{Sa_1}(\rho, H_1)$ and the upper surface to $K^c_{Sa_2}(\rho, H_1)$. Resonance occurs within the region bounded by those two surfaces. For a given pair of parameters $(\hat{\rho}, \hat{H}_1)$, resonance occurs for all K_{Sa} running through the vertical line connecting $K^c_{Sa_1}(\hat{\rho}, \hat{H}_1)$ and $K^c_{Sa_2}(\hat{\rho}, \hat{H}_1)$.

Another manifestation of the surface tension occurs in the coefficients $V^{(2)}_{1,2,3}$ of the amplitude equation (4.16) for type-A resonance. For gravity-capillary waves, the correct coefficients are obtained by replacing the constant g by the modified constant $\hat{g} = g + (\gamma_1/\rho_1)k^2$, in the third and fourth entries of the matrix $\boldsymbol{M}$ defined in Appendix E, as well as in the first entry the matrix $\boldsymbol{G}$ defined in [10].

4.5.2 Special traveling waves when surface tension is taken into account

One can observe from Figure 4.9 (b) that it is possible, when surface tension is present, to find three distinct wavenumbers with equal linear wave speed, and therefore to obtain traveling waves in class-III. Moreover it is clear that they belong to the subset where $\lim_{K\to 0} \Omega_-(K)/K > \min_K \Omega_+(K)/K$. However, the wavenumber subsets where this condition is satisfied depend on the physical parameters, as shown in Figure 4.12. As mentioned in the previous section, a traveling wave for class-III resonance can be found when the triad satisfies

$$\begin{cases} K_{S2} + K_I = K_{S1} & (4.27) \\ \dfrac{\Omega_{S2}}{K_{S2}} = \dfrac{\Omega_I}{K_I} = \dfrac{\Omega_{S1}}{K_{S1}} & (4.28) \end{cases}$$

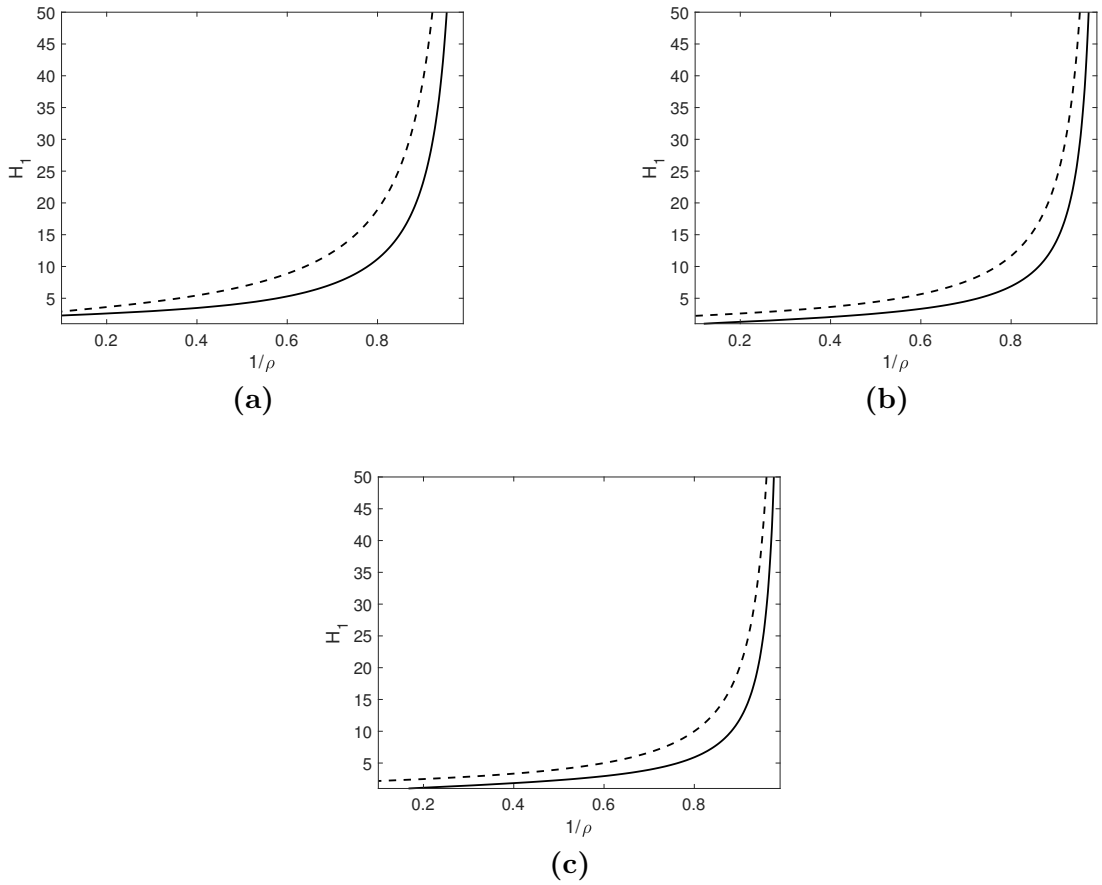

Figure 4.14 Comparaison of resonance (solid) and traveling waves (dashed) parameter region in the (ρ, H_1)-space for (a) $h = 1$, (b) $h = 5$ and (c) $h \to \infty$. The parameter regions lie above the curves.

along with the following amplitude conditions

$$|Z_2|^2 = \frac{K_{S1}}{K_{S2}}|Z_1|^2, \qquad |Z_3|^2 = \frac{K_{S1}}{K_I}|Z_1|^2. \tag{4.29}$$

Traveling waves are special resonant triads and can be found in a limited set of values of the density and depth ratios. Figure 4.14 shows the physical parameter region where traveling waves can be found as a subset of the physical parameter region for resonance.

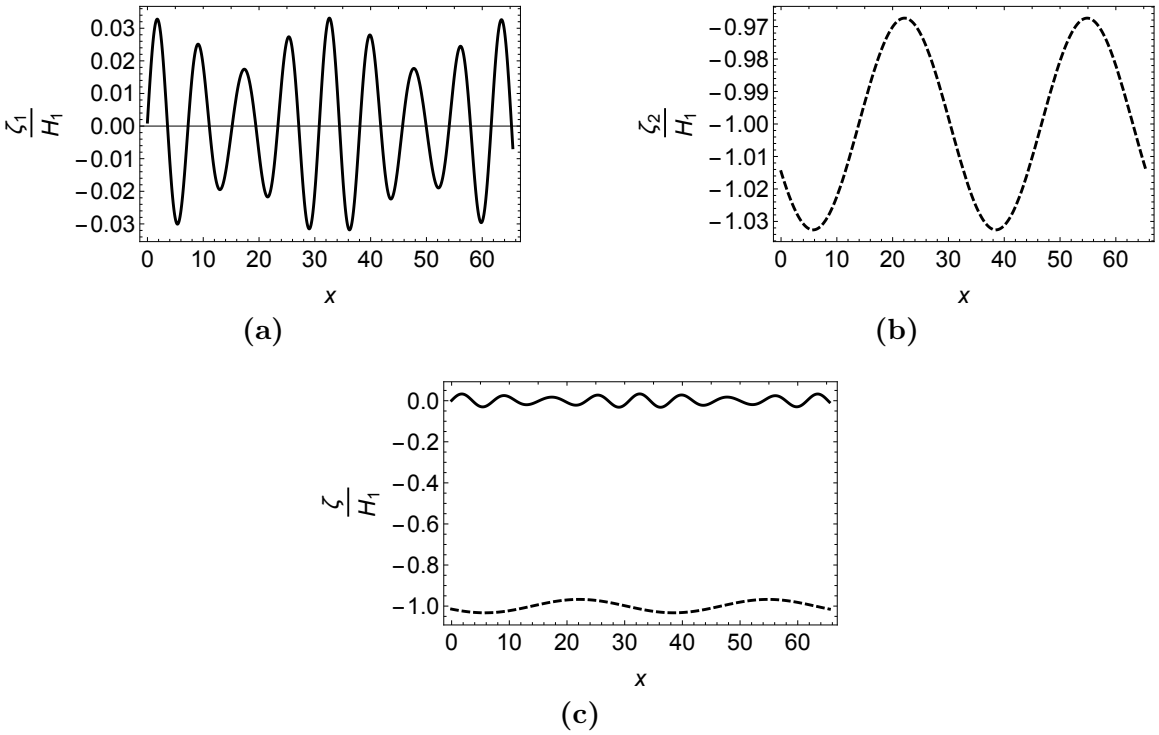

Figure 4.15 Surface elevation for traveling waves in class-III with surface tension resonance with $K_1^+ = 1.01$, $K_2^+ = 0.818$, $K_3^- = 0.192$, $\rho_2/\rho_1 = 1.11$, $|Z_1| = 0.449$, $|Z_2| = 0.499$, $|Z_3| = 1.031$, $H_1 = 45$, $h_2/h_1 = 5$: (a) surface elevation ζ_1; (b) interface elevation ζ_2; (c) both surface (solid) and internal (dashed) elevations.

4.5.3 Example

We give an example below of a traveling wave resulting from the class-III triad resonance with surface tension by finding a numerical solution to equations (4.27)-(4.29). We present in Figure 4.15 the surface and interface elevations, where $K_1^+ = 1.01$, $K_2^+ = 0.818$, $K_3^- = 0.192$, $\rho_2/\rho_1 = 1.11$, and $h_2/h_1 = 5$. In this example, the wave slopes defined as $\varepsilon_S = K_{S1}|a_+|/2\pi$ and $\varepsilon_I = K_I|a_-|/2\pi$ for the upper and lower surface, respectively, are $\varepsilon_S = 0.03$ and $\varepsilon_I = 0.02$. One can observe a spatial modulation of the upper surface, which might be due to the closeness of the two surface wavenumbers. Finally, the surface wave is a short wave, while the internal wave is a long wave, as expected for the class-III resonance.

CHAPTER 5

CONCLUSION

We have first re-examined three-wave resonant interactions of gravity-capillary waves using the amplitude equations derived from a third-order asymptotic model for the weakly nonlinear evolution of surface waves of small steepness proposed by Choi [8]. After having identified the region of resonance, an alternative to the previous representations of resonant wavenumbers and wave frequencies of McGoldrick [19] and Simmons [25] has been proposed in terms of two propagation angles. This could provide a convenient way to understand possible resonant triads. Special attention has been paid to resonant triad interactions in which no energy exchange occurs so that the amplitudes of the triad remain constant during the interactions. The explicit conditions under which interactions with no energy exchange exist have been found, in terms of initial wave amplitudes and phases. Any resonant triad that fails to fulfill the conditions must exchange energy and the amplitudes vary periodically in time. Among constant-amplitude resonant triads, it is shown that all symmetric triads (with one wavenumber vector bisecting the angle between the other two wavenumber vectors) can propagate with a constant wave speed to form a transversely-modulated traveling wave. These special solutions correspond to the fixed points of a system of three ODEs describing the solutions of the triad interaction system. From the resonant triad interaction phase portraits, one can see that all solutions of the system, including the fixed points, are stable. Nevertheless, the linear stability of the solutions subject to more general perturbations remains to be addressed, but is beyond the scope of the present study.

We have then studied 2D resonant triad interactions of two different types between surface and internal wave modes in a system of two layers with different densities. For the type-A resonance, two surface waves and one internal wave

interact resonantly or near resonantly while one surface wave and two internal waves are involved for the type-B resonance. The explicit spectral domain of resonance, including the resonance surface and resonance region, is presented for each type of resonance and its boundaries are identified to represent 1D resonant interactions. Under the type-A resonance conditions given by $\boldsymbol{K}_1^+ = \boldsymbol{K}_2^+ + \boldsymbol{K}_3^-$ and $\Omega_1^+ = \Omega_2^+ + \Omega_3^-$, the resonance region in the (K_2^+, K_3^-)-plane is bounded by the 1D class-I and class-III resonances. On the other hand, under the type-B resonance conditions given by $\boldsymbol{K}_1^+ = \boldsymbol{K}_2^- + \boldsymbol{K}_3^-$ and $\Omega_1^+ = \Omega_2^- + \Omega_3^-$, the resonance region in the (K_2^-, K_3^-)-plane is bounded by the 1D class-II resonances when the density ratio is less than 3. Otherwise, it has been shown that the region is bounded by the class-II and class-IV resonances. Based on the amplitude equation for type-A and type-B triad resonance derived by Choi et al, [10], by using the conditions under which resonant triads exchange no energy during their interaction derived in §3, we have found traveling wave solutions, after matching the linear wave speeds and nonlinear wave speed corrections. It is shown that, for the class-III resonance, such solutions can be found only when surface tension is taken into account. For class-IV resonance that occurs when the density ratio is greater than three, traveling wave solutions of permanent form are found without surface tension, and fall necessarily into Wilton type traveling waves in the sense that $K_S = 2K_I$.

Future work includes (1) finding two-dimensional traveling wave solutions formed by triads in two-layer systems and (2) investigating their stability when they are subject to general perturbations, which can be studied using the Euler equations.

APPENDIX A

COMPUTATION OF THE RIGHT-HAND SIDE OF THE PSEUDO-SPECTRAL EQUATION

We present below the computations of the terms in the right-hand side of Equation (3.17).

$$
\begin{aligned}
&\nabla\Phi^{(1)} \cdot \nabla\zeta^{(1)} = \\
&= \nabla \left(\sum_{j=1}^{3} b_j(\tau,t) E_j + \sum_{j=1}^{3} b_j^*(\tau,t) E_j^* \right) \cdot \nabla \left(\sum_{j=1}^{3} a_j(t) E_j + \sum_{j=1}^{3} a_j^*(\tau,t) E_j^* \right) \\
&= \left(\sum_{j=1}^{3} b_j(\tau,t) \nabla E_j + \sum_{j=1}^{3} b_j^*(\tau,t) \nabla E_j^* \right) \cdot \left(\sum_{j=1}^{3} a_j(\tau,t) \nabla E_j + \sum_{j=1}^{3} a_j^*(\tau,t) \nabla E_j^* \right) \\
&= \left(\sum_{j=1}^{3} b_j(\tau,t) i\underline{k}_j E_j - \sum_{j=1}^{3} b_j^*(\tau,t) i\underline{k}_j E_j^* \right) \cdot \left(\sum_{j=1}^{3} a_j(\tau,t) i\underline{k}_j E_j - \sum_{j=1}^{3} a_j^*(\tau,t) i\underline{k}_j E_j^* \right) \\
&= \left(\sum_{j=1}^{3} b_j(\tau,t) i\underline{k}_j E_j \right) \cdot \left(\sum_{j=1}^{3} a_j(\tau,t) i\underline{k}_j E_j \right) - \left(\sum_{j=1}^{3} b_j(\tau,t) i\underline{k}_j E_j \right) \cdot \left(\sum_{j=1}^{3} a_j^*(\tau,t) i\underline{k}_j E_j^* \right) - \\
&- \left(\sum_{j=1}^{3} b_j^*(\tau,t) i\underline{k}_j E_j^* \right) \cdot \left(\sum_{j=1}^{3} a_j(\tau,t) i\underline{k}_j E_j \right) + \left(\sum_{j=1}^{3} b_j^*(\tau,t) i\underline{k}_j E_j^* \right) \cdot \left(\sum_{j=1}^{3} a_j^*(\tau,t) i\underline{k}_j E_j^* \right) \\
&= \left(\sum_{j=1}^{3} b_j(\tau,t) i k_{j,x} E_j \right) \left(\sum_{j=1}^{3} a_j(\tau,t) i k_{j,x} E_j \right) + \left(\sum_{j=1}^{3} b_j(\tau,t) i k_{j,y} E_j \right) \left(\sum_{j=1}^{3} a_j(\tau,t) i k_{j,y} E_j \right) - \\
&- \left(\sum_{j=1}^{3} b_j(\tau,t) i k_{j,x} E_j \right) \left(\sum_{j=1}^{3} a_j^*(\tau,t) i k_{j,x} E_j^* \right) - \left(\sum_{j=1}^{3} b_j(\tau,t) i k_{j,y} E_j \right) \left(\sum_{j=1}^{3} a_j^*(\tau,t) i k_{j,y} E_j^* \right) - \\
&- \left(\sum_{j=1}^{3} b_j^*(\tau,t) i k_{j,x} E_j^* \right) \left(\sum_{j=1}^{3} a_j(\tau,t) i k_{j,x} E_j \right) - \left(\sum_{j=1}^{3} b_j^*(\tau,t) i k_{j,y} E_j^* \right) \left(\sum_{j=1}^{3} a_j(\tau,t) i k_{j,y} E_j \right) + \\
&+ \left(\sum_{j=1}^{3} b_j^*(\tau,t) i k_{j,x} E_j^* \right) \left(\sum_{j=1}^{3} a_j^*(\tau,t) i k_{j,x} E_j^* \right) + \left(\sum_{j=1}^{3} b_j^*(\tau,t) i k_{j,y} E_j^* \right) \left(\sum_{j=1}^{3} a_j^*(\tau,t) i k_{j,y} E_j^* \right).
\end{aligned}
$$

$$\begin{aligned}
\zeta^{(1)}\Delta\Phi^{(1)} &= \left(\sum_{j=1}^{3} a_j(\tau,t)E_j + \sum_{j=1}^{3} a_j^*(\tau,t)E_j^*\right)\Delta\left(\sum_{j=1}^{3} b_j(\tau,t)E_j + \sum_{j=1}^{3} b_j^*(\tau,t)E_j^*\right)\\
&= \left(\sum_{j=1}^{3} a_j(\tau,t)E_j + \sum_{j=1}^{3} a_j^*(\tau,t)E_j^*\right)\left(\sum_{j=1}^{3} b_j(\tau,t)\Delta E_j + \sum_{j=1}^{3} b_j^*(\tau,t)\Delta E_j^*\right)\\
&= -\left(\sum_{j=1}^{3} a_j(\tau,t)E_j + \sum_{j=1}^{3} a_j^*(\tau,t)E_j^*\right)\left(\sum_{j=1}^{3} b_j(\tau,t)k_j^2E_j + \sum_{j=1}^{3} b_j^*(\tau,t)k_j^2E_j^*\right).
\end{aligned}$$

$$\begin{aligned}
\mathcal{L}[\zeta^{(1)}\mathcal{L}[\Phi^{(1)}]] &= \mathcal{L}\left[\left(\sum_{j=1}^{3} a_j(\tau,t)E_j + \sum_{j=1}^{3} a_j^*(\tau,t)E_j^*\right)\mathcal{L}\left[\sum_{j=1}^{3} b_j(\tau,t)E_j + \sum_{j=1}^{3} b_j^*(\tau,t)E_j^*\right]\right]\\
&= -\mathcal{L}\left[\left(\sum_{j=1}^{3} a_j(\tau,t)E_j + \sum_{j=1}^{3} a_j^*(\tau,t)E_j^*\right)\left(\sum_{j=1}^{3} b_j(\tau,t)k_jE_j + \sum_{j=1}^{3} b_j^*(\tau,t)k_jE_j^*\right)\right]\\
&= -\sum_{j=1}^{3} a_j(\tau,t)\mathcal{L}[E_j\sum_{l=1}^{3} b_l(\tau,t)k_lE_l] - \sum_{j=1}^{3} a_j(\tau,t)\mathcal{L}[E_j\sum_{l=1}^{3} b_l^*(\tau,t)k_lE_l^*] -\\
&- \sum_{j=1}^{3} a_j^*(\tau,t)\mathcal{L}[E_j^*\sum_{l=1}^{3} b_l(\tau,t)k_lE_l] - \sum_{j=1}^{3} a_j^*(\tau,t)\mathcal{L}[E_j^*\sum_{l=1}^{3} b_l^*(\tau,t)k_lE_l^*]\\
&= -\sum_{j=1}^{3}\sum_{l=1}^{3} a_j(\tau,t)b_l(\tau,t)k_l\mathcal{L}[E_jE_l] - \sum_{j=1}^{3}\sum_{l=1}^{3} a_j(\tau,t)b_l^*(\tau,t)k_l\mathcal{L}[E_jE_l^*] -\\
&- \sum_{j=1}^{3}\sum_{l=1}^{3} a_j^*(\tau,t)b_l(\tau,t)k_l\mathcal{L}[E_j^*E_l] - \sum_{j=1}^{3}\sum_{l=1}^{3} a_j^*(\tau,t)b_l^*(\tau,t)k_l\mathcal{L}[E_j^*E_l^*]\\
&= \sum_{j=1}^{3}\sum_{l=1}^{3} a_j(\tau,t)b_l(\tau,t)k_l|\underline{k}_j + \underline{k}_l|E_{j+l} + \sum_{j=1}^{3}\sum_{l=1}^{3} a_j(\tau,t)b_l^*(\tau,t)k_l|\underline{k}_j - \underline{k}_l|E_{j-l} +\\
&+ \sum_{j=1}^{3}\sum_{l=1}^{3} a_j^*(\tau,t)b_l(\tau,t)k_l|-\underline{k}_j + \underline{k}_l|E_{-j+l} + \sum_{j=1}^{3}\sum_{l=1}^{3} a_j^*(\tau,t)b_l^*(\tau,t)k_l|\underline{k}_j + \underline{k}_l|E_{-(j+l)}.
\end{aligned}$$

$$
\begin{aligned}
|\nabla\Phi^{(1)}|^2 &= \left|\nabla\left(\sum_{j=1}^{3} b_j(\tau,t)E_j + \sum_{j=1}^{3} b_j^*(\tau,t)E_j^*\right)\right|^2 \\
&= \left|\left(\sum_{j=1}^{3} b_j(\tau,t)\nabla E_j + \sum_{j=1}^{3} b_j^*(\tau,t)\nabla E_j^*\right)\right|^2 \\
&= \left|\left(\sum_{j=1}^{3} b_j(\tau,t)i\underline{k}_j E_j - \sum_{j=1}^{3} b_j^*(\tau,t)i\underline{k}_j E_j^*\right)\right|^2 \\
&= \left(\sum_{j=1}^{3} b_j(\tau,t)i\underline{k}_j E_j - \sum_{j=1}^{3} b_j^*(\tau,t)i\underline{k}_j E_j^*\right)\cdot\left(\sum_{j=1}^{3} b_j(\tau,t)i\underline{k}_j E_j - \sum_{j=1}^{3} b_j^*(\tau,t)i\underline{k}_j E_j^*\right) \\
&= \left(\sum_{j=1}^{3} b_j(\tau,t)ik_{j,x}E_j\right)^2 + \left(\sum_{j=1}^{3} b_j(\tau,t)ik_{j,y}E_j\right)^2 \\
&- 2\left(\sum_{j=1}^{3} b_j(\tau,t)ik_{j,x}E_j\right)\left(\sum_{j=1}^{3} b_j^*(\tau,t)ik_{j,x}E_j^*\right) \\
&- 2\left(\sum_{j=1}^{3} b_j(\tau,t)ik_{j,y}E_j\right)\left(\sum_{j=1}^{3} b_j^*(\tau,t)ik_{j,y}E_j^*\right) + \\
&\left(\sum_{j=1}^{3} b_j^*(\tau,t)ik_{j,x}E_j^*\right)^2 + \left(\sum_{j=1}^{3} b_j^*(\tau,t)ik_{j,y}E_j^*\right)^2.
\end{aligned}
$$

$$
\begin{aligned}
(\mathcal{L}[\Phi^{(1)}])^2 &= \left(\mathcal{L}[\sum_{j=1}^{3} b_j(\tau,t)E_j + \sum_{j=1}^{3} b_j^*(\tau,t)E_j^*]\right)^2 \\
&= \left(\sum_{j=1}^{3} b_j(\tau,t)\mathcal{L}[E_j] + \sum_{j=1}^{3} b_j^*(\tau,t)\mathcal{L}[E_j^*]\right)^2 \\
&= \left(\sum_{j=1}^{3} b_j(\tau,t)k_j E_j + \sum_{j=1}^{3} b_j^*(\tau,t)k_j E_j^*\right)^2.
\end{aligned}
$$

APPENDIX B

RESCALING OF THE COEFFICIENT IN THE REDUCED MODEL

We present here how the coefficients of Equation (3.19) can be rescaled to one. Let us set $A_j = c_j \tilde{A}_j$ (j=1,2,3), where $c_j \in \mathbb{R}$ and $A_j \in \mathbb{C}$. Inserting these in the reduced model (3.19) allows to write it as

$$\frac{\mathrm{d}\tilde{A}_1}{\mathrm{d}\tau} = \mathrm{i}\,\Gamma_0\,\tilde{A}_2\tilde{A}_3\,, \quad \frac{\mathrm{d}\tilde{A}_2}{\mathrm{d}\tau} = \mathrm{i}\,\Gamma_0\,\tilde{A}_3^*\tilde{A}_1\,, \quad \frac{\mathrm{d}\tilde{A}_3}{\mathrm{d}\tau} = \mathrm{i}\,\Gamma_0\,\tilde{A}_1\tilde{A}_2^*\,, \tag{B.1}$$

provided

$$c_1 = \sqrt{\frac{\Gamma_1}{\Gamma_2}}c_2\,, \quad c_3 = \sqrt{\frac{\Gamma_3}{\Gamma_1}}c_1\,, \quad \Gamma_0 = c_2\sqrt{\Gamma_2\Gamma_3}\,. \tag{B.2}$$

Moreover, after introducing a rescaled time $T = \Gamma_0\tau$ we obtain, after dropping the tilde, the system

$$\frac{\mathrm{d}A_1}{\mathrm{d}T} = \mathrm{i}\,A_2A_3\,, \quad \frac{\mathrm{d}A_2}{\mathrm{d}T} = \mathrm{i}\,A_3^*A_1\,, \quad \frac{\mathrm{d}A_3}{\mathrm{d}T} = \mathrm{i}\,A_1A_2^*\,. \tag{B.3}$$

APPENDIX C

THIRD-DEGREE POLYNOMIAL DISCRIMINANT

We present here the calculations of the discriminants of the third-degree polynomials given in Equations (3.52)-(3.54).

- Polynomial in (3.52):

  We set $y = |A_1|^2$, then $y^3 - 2\Gamma_1\mathcal{L}y^2 + \Gamma_1^2\mathcal{L}^2y - \frac{\Gamma_1^2}{\Gamma_2^2}\mathcal{L}_\Delta^2 = 0$ can be written as $x^3 + px + q = 0$ where $y = x + \frac{2}{3}\Gamma_1\mathcal{L}$, $p = -\frac{1}{3}\Gamma_1^2\mathcal{L}^2$ and $q = 2\left(\frac{\Gamma_1\mathcal{L}}{3}\right)^3 - \left(\frac{\Gamma_1\mathcal{L}_\Delta}{\Gamma_2}\right)^2$. Therefore the discriminant is $\Xi_1 = -\left(\frac{\Gamma_1\mathcal{L}_\Delta}{\Gamma_2}\right)^2\left[4\left(\frac{\Gamma_1\mathcal{L}}{3}\right)^3 - \left(\frac{\Gamma_1\mathcal{L}_\Delta}{\Gamma_2}\right)^2\right]$. Therefore we need $0 \leq \mathcal{L}_\Delta^2 \leq \frac{4}{27}\Gamma_1\Gamma_2^2\mathcal{L}^3$.

- Polynomial in (3.53):

  We set $y = |A_2|^2$, then $y^3 - \Gamma_2\mathcal{L}y^2 + \frac{\Gamma_2}{\Gamma_1}\mathcal{L}_\Delta^2 = 0$ can be written as $x^3 + px + q = 0$ where $y = x + \frac{\Gamma_2\mathcal{L}}{3}$, $p = -\frac{(\Gamma_2\mathcal{L})^2}{3}$ and $q = -2\left(\frac{\Gamma_2\mathcal{L}}{3}\right)^3 + \frac{\Gamma_2}{\Gamma_1}\mathcal{L}_\Delta^2$. Then the discriminant is $\Xi_2 = \frac{\Gamma_2}{\Gamma_1}\mathcal{L}_\Delta^2\left[\frac{\Gamma_2}{\Gamma_1}\mathcal{L}_\Delta^2 - 4\left(\frac{\Gamma_2\mathcal{L}}{3}\right)^3\right]$. Therefore we need $0 \leq \mathcal{L}_\Delta^2 \leq \frac{4}{27}\Gamma_1\Gamma_2^2\mathcal{L}^3$.

- Polynomial in (3.54):

  We set $y = |A_3|^2$, then $y^3 - \Gamma_3\mathcal{L}y^2 + \frac{\Gamma_3}{\Gamma_1}\mathcal{L}_\Delta^2 = 0$ can be written as $x^3 + px + q = 0$ where $y = x + \frac{\Gamma_3\mathcal{L}}{3}$, $p = -\frac{(\Gamma_3\mathcal{L})^2}{3}$ and $q = -2\left(\frac{\Gamma_3\mathcal{L}}{3}\right)^3 + \frac{\Gamma_3}{\Gamma_1}\mathcal{L}_\Delta^2$. Then the discriminant is $\Xi_3 = \frac{\Gamma_3}{\Gamma_1}\mathcal{L}_\Delta^2\left[\frac{\Gamma_3}{\Gamma_1}\mathcal{L}_\Delta^2 - 4\left(\frac{\Gamma_3\mathcal{L}}{3}\right)^3\right]$. Therefore we need $0 \leq \mathcal{L}_\Delta^2 \leq \frac{4}{27}\Gamma_1\Gamma_3^2\mathcal{L}^3$.

APPENDIX D

PLOTS OF GROUP VELOCITY FUNCTIONS FOR DIFFERENT CASES

We present here the graphs of the group velocities of surface and internal wave modes.

In all the plots below, the physical parameters have been arbitrarily chosen.

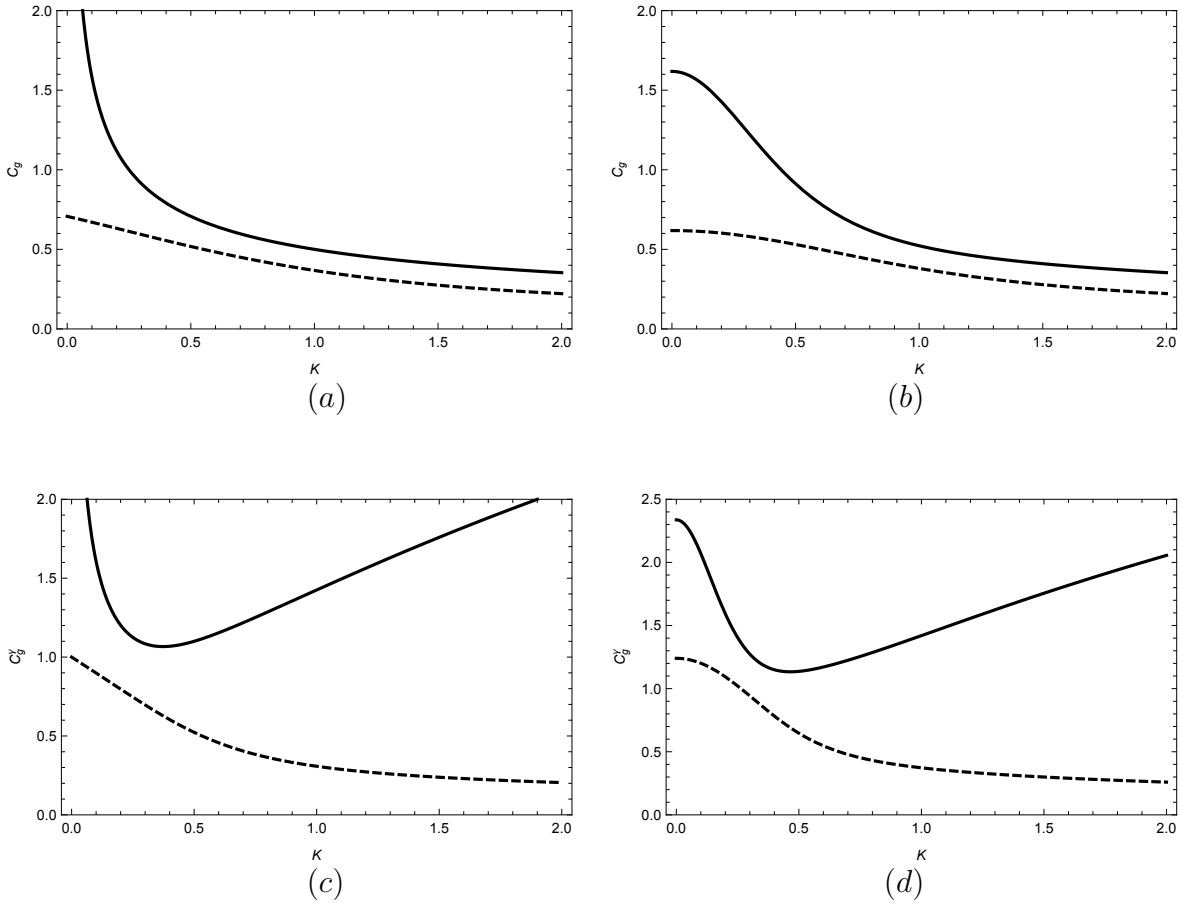

Figure D.1 Group velocity when surface tension is absent for (a) infinite depth, (b) finite depth. Group velocity when surface tension is present for (c) infinite depth (d) finite depth.

APPENDIX E

INTERACTION COEFFICIENTS

We present here the interaction coefficients of Equations (4.16)-(4.17). As detailed in [10], the coefficients $U^{(n)}_{1,2,3}$ $(n = 1, ..., 6)$ are given by

$$\begin{aligned} U^{(1)}_{1,2,3} &= h^{(1)}_{1,2,3} P^{(1,1)}_1 P^{(1,1)}_2 Q^{(1,1)}_3 + h^{(2)}_{1,2,3} P^{(1,1)}_1 P^{(2,1)}_2 Q^{(1,1)}_3 + h^{(3)}_{1,2,3} P^{(2,1)}_1 P^{(2,1)}_2 Q^{(1,1)}_3 \\ &+ h^{(4)}_{1,2,3} P^{(1,1)}_1 P^{(1,1)}_2 Q^{(2,1)}_3 + h^{(5)}_{1,2,3} P^{(1,1)}_1 P^{(2,1)}_2 Q^{(2,1)}_3 + h^{(6)}_{1,2,3} P^{(2,1)}_1 P^{(2,1)}_2 Q^{(2,1)}_3, \end{aligned}$$

$$\begin{aligned} U^{(2)}_{1,2,3} &= 2h^{(1)}_{1,2,3} P^{(1,1)}_1 P^{(1,2)}_2 Q^{(1,1)}_3 + h^{(2)}_{1,2,3} P^{(1,1)}_1 P^{(2,2)}_2 Q^{(1,1)}_3 + h^{(2)}_{2,1,3} P^{(2,1)}_1 P^{(1,2)}_2 Q^{(1,1)}_3 \\ &+ 2h^{(3)}_{1,2,3} P^{(2,1)}_1 P^{(2,2)}_2 Q^{(1,1)}_3 + 2h^{(4)}_{1,2,3} P^{(1,1)}_1 P^{(1,2)}_2 Q^{(2,1)}_3 \\ &+ h^{(5)}_{1,2,3} P^{(1,1)}_1 P^{(2,2)}_2 Q^{(2,1)}_3 + h^{(5)}_{2,1,3} P^{(2,1)}_1 P^{(1,2)}_2 Q^{(2,1)}_3 + 2h^{(6)}_{1,2,3} P^{(2,1)}_1 P^{(2,2)}_2 Q^{(2,1)}_3, \end{aligned}$$

$$\begin{aligned} U^{(3)}_{1,2,3} &= h^{(1)}_{1,2,3} P^{(1,2)}_1 P^{(1,2)}_2 Q^{(1,1)}_3 + h^{(2)}_{1,2,3} P^{(1,2)}_1 P^{(2,2)}_2 Q^{(1,1)}_3 + h^{(3)}_{1,2,3} P^{(2,2)}_1 P^{(2,2)}_2 Q^{(1,1)}_3 \\ &+ h^{(4)}_{1,2,3} P^{(1,2)}_1 P^{(1,2)}_2 Q^{(2,1)}_3 + h^{(5)}_{1,2,3} P^{(1,2)}_1 P^{(1,2)}_2 Q^{(2,1)}_3 + h^{(6)}_{1,2,3} P^{(2,2)}_1 P^{(2,2)}_2 Q^{(2,2)}_3, \end{aligned}$$

$$\begin{aligned} U^{(4)}_{1,2,3} &= h^{(1)}_{1,2,3} P^{(1,1)}_1 P^{(1,1)}_2 Q^{(1,2)}_3 + h^{(2)}_{1,2,3} P^{(1,1)}_1 P^{(2,1)}_2 Q^{(1,2)}_3 + h^{(3)}_{1,2,3} P^{(2,1)}_1 P^{(2,1)}_2 Q^{(1,2)}_3 \\ &+ h^{(4)}_{1,2,3} P^{(1,1)}_1 P^{(1,1)}_2 Q^{(2,2)}_3 + h^{(5)}_{1,2,3} P^{(1,1)}_1 P^{(2,1)}_2 Q^{(2,2)}_3 + h^{(6)}_{1,2,3} P^{(2,1)}_1 P^{(2,1)}_2 Q^{(2,2)}_3, \end{aligned}$$

$$U^{(5)}_{1,2,3} = 2h^{(1)}_{1,2,3}P^{(1,1)}_1 P^{(1,2)}_2 Q^{(1,2)}_3 + h^{(2)}_{1,2,3}P^{(1,1)}_1 P^{(2,2)}_2 Q^{(1,2)}_3 + h^{(2)}_{2,1,3}P^{(2,1)}_1 P^{(1,2)}_2 Q^{(1,2)}_3$$
$$+ 2h^{(3)}_{1,2,3}P^{(2,1)}_1 P^{(2,2)}_2 Q^{(1,2)}_3 + 2h^{(4)}_{1,2,3}P^{(1,1)}_1 P^{(1,2)}_2 Q^{(2,2)}_3$$
$$+ h^{(5)}_{1,2,3}P^{(1,1)}_1 P^{(2,2)}_2 Q^{(2,2)}_3 + h^{(5)}_{2,1,3}P^{(2,1)}_1 P^{(1,2)}_2 Q^{(2,2)}_3 + 2h^{(6)}_{1,2,3}P^{(2,1)}_1 P^{(2,2)}_2 Q^{(2,2)}_3,$$

$$U^{(6)}_{1,2,3} = h^{(1)}_{1,2,3}P^{(1,2)}_1 P^{(1,2)}_2 Q^{(1,2)}_3 + h^{(2)}_{1,2,3}P^{(1,2)}_1 P^{(2,2)}_2 Q^{(1,2)}_3 + h^{(3)}_{1,2,3}P^{(2,2)}_1 P^{(2,2)}_2 Q^{(1,2)}_3$$
$$+ h^{(4)}_{1,2,3}P^{(1,2)}_1 P^{(1,2)}_2 Q^{(2,2)}_3 + h^{(5)}_{1,2,3}P^{(1,2)}_1 P^{(2,2)}_2 Q^{(2,2)}_3 + h^{(6)}_{1,2,3}P^{(2,2)}_1 P^{(2,2)}_2 Q^{(2,2)}_3,$$

where $h^{(n)}_{1,2,3}$ are defined by

$$h^{(1)}_{1,2,3} = \frac{1}{2}\left(\boldsymbol{k}_1 \cdot \boldsymbol{k}_2\right)/\rho_1 - \frac{1}{2}\rho_1\gamma_{11,1}\gamma_{12,2} \tag{E.1}$$

$$h^{(2)}_{1,2,3} = -\rho_1\gamma_{11,1}\gamma_{12,2}, \quad h^{(3)}_{1,2,3} = -\frac{1}{2}\rho_1\gamma_{12,1}\gamma_{12,2}, \tag{E.2}$$

$$h^{(4)}_{1,2,3} = -\frac{1}{2}\Delta\rho\left[(\rho_2/\rho_1)\gamma_{31,1}\gamma_{31,2}\left(\boldsymbol{k}_1 \cdot \boldsymbol{k}_2\right) + \gamma_{21,1}\gamma_{21,2}\right], \tag{E.3}$$

$$h^{(5)}_{1,2,3} = -\Delta\rho\gamma_{21,1}\gamma_{22,2} - \rho_2\gamma_{31,1}\gamma_{33,2}\left(\boldsymbol{k}_1 \cdot \boldsymbol{k}_2\right), \tag{E.4}$$

$$h^{(6)}_{1,2,3} = -\frac{1}{2}\left[\Delta\rho\gamma_{22,1}\gamma_{22,2} + \left(\rho_2\gamma_{30,1}\gamma_{30,2} - \rho_1\gamma_{32,1}\gamma_{32,2}\right)\left(\boldsymbol{k}_1 \cdot \boldsymbol{k}_2\right)\right], \tag{E.5}$$

where $\gamma_{mn,j}$ denote γ_{mn} defined in (F.7)-(F.8) with $k = k_j$ so that

$$\gamma_{11,j} = k_j J_j \left[(\rho_2/\rho_1)U_j + L_j\right], \quad \gamma_{12,j} = \gamma_{21,j} = k_j J_j S_j L_j, \quad \gamma_{22,j} = k_j J_j L_j, \tag{E.6}$$

$$\gamma_{30,j} = J_j, \quad \gamma_{31,j} J_j S_j, \quad \gamma_{32,j} = J_j U_j L_j, \quad \gamma_{33,j} = J_j \left(1 + U_j L_j\right). \tag{E.7}$$

Note that $h^{(j)}_{1,2,3}$ verifies $h^{(j)}_{1,2,3} = h^{(j)}_{2,1,3}$ for $j = 1, 3, 4, 6$. In addition, $Q^{(i,j)}$ are the entries of the matrix defined in (F.2), and $P^{(i,j)}$ are the elements of the matrix defined by

$$\boldsymbol{P} = \boldsymbol{\Gamma}^{-1} \boldsymbol{M} \boldsymbol{S}^{1/2}, \tag{E.8}$$

where $\boldsymbol{M}$ and $\boldsymbol{S}$ are two matrices defined in Appendix F, and where $\boldsymbol{\Gamma}$ is given by

$$\boldsymbol{\Gamma} = \begin{pmatrix} \gamma_{11} & \gamma_{12} \\ \gamma_{21} & \gamma_{22} \end{pmatrix}. \tag{E.9}$$

After defining $\bar{U}^n_{1,2,3}$ $(n = 1, ..., 6)$ as

$$\bar{U}^{(1)}_{1,2,3} = -\sqrt{\frac{\omega_1^+ \omega_2^+}{8\omega_3^+}} U^{(1)}_{1,2,3}, \quad \bar{U}^{(2)}_{1,2,3} = -\sqrt{\frac{\omega_1^+ \omega_2^-}{8\omega_3^+}} U^{(2)}_{1,2,3}, \quad \bar{U}^{(3)}_{1,2,3} = -\sqrt{\frac{\omega_1^- \omega_2^-}{8\omega_3^-}} U^{(3)}_{1,2,3},$$

$$\bar{U}^{(4)}_{1,2,3} = -\sqrt{\frac{\omega_1^+ \omega_2^+}{8\omega_3^-}} U^{(4)}_{1,2,3}, \quad \bar{U}^{(5)}_{1,2,3} = -\sqrt{\frac{\omega_1^+ \omega_2^-}{8\omega_3^-}} U^{(5)}_{1,2,3}, \quad \bar{U}^{(6)}_{1,2,3} = -\sqrt{\frac{\omega_1^- \omega_2^-}{8\omega_3^-}} U^{(6)}_{1,2,3},$$

the coefficients $V^{(n)}_{1,2,3}$ $(n = 1, ..., 6)$ of the amplitude equations (4.16)-(4.16) are given by

$$V^{(1)}_{1,2,3} = \bar{U}^{(1)}_{2,3,-1} - \bar{U}^{(1)}_{-1,2,3} - \bar{U}^{(1)}_{3,-1,2}, \quad V^{(2)}_{1,2,3} = -\bar{U}^{(2)}_{-1,3,2} + \bar{U}^{(2)}_{2,3,-1} - \bar{U}^{(4)}_{-1,2,3} - \bar{U}^{(4)}_{2,-1,3},$$

$$V^{(3)}_{1,2,3} = -\bar{U}^{(2)}_{3,-1,2} + \bar{U}^{(4)}_{2,3,-1}, \quad V^{(4)}_{1,2,3} = -\bar{U}^{(3)}_{-1,2,3} - \bar{U}^{(3)}_{2,-1,3} + \bar{U}^{(5)}_{3,2,-1} - \bar{U}^{(5)}_{3,-1,2},$$

$$V^{(5)}_{1,2,3} = \bar{U}^{(3)}_{2,3,-1} - \bar{U}^{(5)}_{-1,2,3}, \quad V^{(6)}_{1,2,3} = \bar{U}^{(6)}_{2,3,-1} - \bar{U}^{(6)}_{-1,2,3} - \bar{U}^{(6)}_{3,-1,2},$$

$$V^{(7)}_{1,2,3} = \bar{U}^{(1)}_{1,2,3}, \quad V^{(8)}_{1,2,3} = \bar{U}^{(2)}_{1,3,2} + \bar{U}^{(4)}_{1,3,2}, \quad V^{(9)}_{1,2,3} = \bar{U}^{(3)}_{2,3,1} + \bar{U}^{(5)}_{1,2,3}, \quad V^{(10)}_{1,2,3} = \bar{U}^{(6)}_{1,2,3}.$$

APPENDIX F

DEFINITIONS OF SURFACE AND INTERFACE ELEVATIONS

We present here how the surface and internal elevations ζ_1 and ζ_2 are recovered from the wave amplitudes $\mathcal{A}_j$ and $\mathcal{B}_j$ $(j = 1, 2, 3)$. Following [10], the surface and internal elevations ζ_1 and ζ_2 are defined as

$$\zeta_1(\boldsymbol{x}, t) = \sum_{j=1}^{3} a_+(\boldsymbol{k}_j, t)\mathrm{e}^{-\mathrm{i}\boldsymbol{k}_j\cdot\boldsymbol{x}} + \text{C.C.}\,, \qquad \zeta_2(\boldsymbol{x}, t) = \sum_{j=1}^{3} a_-(\boldsymbol{k}_j, t)\mathrm{e}^{-\mathrm{i}\boldsymbol{k}_j\cdot\boldsymbol{x}} + \text{C.C.}\,, \tag{F.1}$$

where $\boldsymbol{a} = (a_+, a_-)^T \in \mathbb{C}^2$ is defined by the relations

$$\boldsymbol{a} = \boldsymbol{Q}\boldsymbol{q}\,, \qquad \boldsymbol{Q} = \boldsymbol{M}\boldsymbol{S}^{1/2}. \tag{F.2}$$

The complex valued vector $\boldsymbol{q} = (q_+, q_-)^T$ is defined as

$$q_+(\boldsymbol{k}, t) = \sqrt{\frac{1}{2\omega_+}}\left[Y(\boldsymbol{k}, t) + Y^*(-\boldsymbol{k}, t)\right]\,, \qquad q_-(\boldsymbol{k}, t) = \sqrt{\frac{1}{2\omega_+}}\left[Z(\boldsymbol{k}, t) + Z^*(-\boldsymbol{k}, t)\right]\,, \tag{F.3}$$

where ω_+ and ω_- represent the surface and internal wave dispersion relations, respectively, and

$$Y(\boldsymbol{k}, t) = \mathcal{A}(\boldsymbol{k}, t)\mathrm{e}^{\mathrm{i}\omega_+ t}\,, \qquad Z(\boldsymbol{k}, t) = \mathcal{B}(\boldsymbol{k}, t)\mathrm{e}^{\mathrm{i}\omega_- t}\,. \tag{F.4}$$

The matrix $\boldsymbol{M}$ is defined as

$$\boldsymbol{M} = \begin{pmatrix} \omega_+^2 - \Delta\rho g\gamma_{22} & \Delta\rho g\gamma_{12} \\ \rho_1 g\gamma_{21} & \omega_-^2 - \rho_1 g\gamma_{11} \end{pmatrix} \begin{pmatrix} n_+ & 0 \\ 0 & n_- \end{pmatrix}, \tag{F.5}$$

where $\Delta\rho = \rho_2 - \rho_1$, and n_+ and n_- are given by

$$n_+ = \left[(\omega_+^2 - \Delta\rho\gamma_{22})^2 + (\rho_1 g\gamma_{21})^2\right]^{-1/2}, \quad n_- = \left[(\omega_-^2 - \rho_1 g\gamma_{11})^2 + (\rho_1 g\gamma_{21})^2\right]^{1/2}. \tag{F.6}$$

The coefficients γ's are defined as

$$\gamma_{11} = kJ\left[(\rho_2/\rho_1)T_1 + T_2\right], \quad \gamma_{12} = \gamma_{21} = kJST_2, \quad \gamma_{22} = kJT_2, \tag{F.7}$$

$$\gamma_{31} = JS, \quad \gamma_{32} = JT_1T_2, \quad \gamma_{33} = J(1 + T_1T_2), \tag{F.8}$$

with J, T_i $(i = 1, 2)$, and S given by

$$T_i = \tanh kh_i, \quad S = \operatorname{sech} kh_1, \quad J = (\rho_1 T_1 T_2 + \rho_2)^{-1}. \tag{F.9}$$

The matrix $\boldsymbol{S}$ is defined as $\boldsymbol{S} = \operatorname{diag}(s_+, s-)$ where

$$s_+ = \frac{1}{n_+^2} \frac{\left[(\rho_1\gamma_{11}^2 - \Delta\rho\gamma_{11}\gamma_{22} + 2\Delta\rho\gamma_{12}^2)\,\omega_+^2 - \Delta\rho g\,(\rho_1\gamma_{11} - \Delta\rho\gamma_{22})\,(\gamma_{11}\gamma_{22} - \gamma_{12}^2)\right]}{g\left[\rho_1\gamma_{11}\omega_+^2 - \Delta\rho\gamma_{22}\omega_-^2 - 2\rho_1\Delta\rho g\,(\gamma_{11}\gamma_{22} - \gamma_{12}^2)\right]^2},$$

$$s_- = \frac{1}{n_-^2} \frac{\left[(\Delta\rho\gamma_{22}^2 - \rho_1\gamma_{11}\gamma_{22} + 2\rho_1\gamma_{12}^2)\,\omega_-^2 + \rho_1 g\,(\rho_1\gamma_{11} - \Delta\rho\gamma_{22})\,(\gamma_{11}\gamma_{22} - \gamma_{12}^2)\right]}{g\left[\rho_1\gamma_{11}\omega_+^2 - \Delta\rho\gamma_{22}\omega_-^2 - 2\rho_1\Delta\rho g\,(\gamma_{11}\gamma_{22} - \gamma_{12}^2)\right]^2}.$$

REFERENCES

[1] M-R. Alam, *A new triad resonance between co-propagating surface and interfacial waves*, Journal of Fluid Mechanics, vol. 691, p. 267-278 (2012).

[2] F. K. Ball, *Energy transfer between external and internal gravity waves*, Journal of Fluid Mechanics, vol. 19, p. 465 (1964).

[3] D. J. Benney, *Non-linear gravity wave interactions*, Journal of Fluid Mechanics, vol. 14, p. 577-584 (1962).

[4] D. J. Benney and A. C. Newell, *The propagation of nonlinear wave envelopes*, Journal of Mathematical Physics, vol. 46, p. 133-139 (1967).

[5] O. Bühler, K. R. Helfrich, *2009 Program of Study: Nonlinear Waves. Technical Report* Woods Hole Oceanographic Institution, Woods Hole, Massachusetts (2010).

[6] K. M. Case and S. C. Chiu, *Three-wave resonant interactions of gravity-capillary waves*, The Physics of Fluids, vol. 20, no. 5 (1976).

[7] M. Chabane and W. Choi, *On resonant interactions of gravity-capillary waves without energy exchange*, Studies in Applied Mathematics, vol. 142, issue 4, p. 528-550 (2019).

[8] W. Choi, *Nonlinear evolution equations for two-dimensional waves in a fluid of finite depth*, Journal of Fluid Mechanics, vol. 295, p. 381-394 (1995).

[9] W. Choi and R. Camassa, *Weakly nonlinear internal waves in a two-fluid system*, Journal of Fluid Mechanics, vol. 313, p. 83-103 (1996).

[10] W. Choi, M. Chabane, T.M.A. Taklo, *Two-dimensional resonant triad interactions in a two-layer system*, submitted to Journal of Fluid Mechanics (2020).

[11] M. Funakoshi, M. Oikawa,*The resonant interaction between a long internal gravity wave and a surface gravity wave packet*, J. Phys. Soc. Japan 52, p. 1982-1995. (1983).

[12] Y. Hashizume, *Interaction between short surface waves and long internal waves*, J. Phys. Soc. Japan 48, p. 631-638 (1980).

[13] J. L. Hammack and D. M. Henderson, *Resonant interactions among surface water waves*, Annu. Rev. Fluid Mech., 25: p. 55-97 (1993).

[14] D. F. Hill and M. A. Foda, *Subharmonic resonance of short internal standing waves by progressive surface waves*, Journal of Fluid Mechanics, vol. 321, p. 217-233 (1996).

[15] T. M. Joyce, *Nonlinear interactions among standing surface and internal gravity waves*, Journal of Fluid Mechanics, vol. 63, part 4, p. 801-825 (1974).

[16] T. Kodaira, T. Waseda, M. Miyata and W. Choi, *Internal solitary waves in a two-fluid system with a free surface*, Journal of Fluid Mechanics, vol. 804, p. 201-223 (1974).

[17] J. E. Lewis, B. M. Lake, D. R. S. Ko, *On the interaction of internal waves and surface gravity waves*, Journal of Fluid Mechanics, vol. 63, p. 773-800 (1974).

[18] M. S. Longuet-Higgins and N. D. Smith, *An experiment on third-order resonant wave interactions*, Journal of Fluid Mechanics, vol. 25, part 3, p. 417-435 (1966).

[19] L. F. McGoldrick, *Resonant interactions among capillary-gravity waves*, Journal of Fluid Mechanics, vol. 21, part 2, p. 305-331 (1965).

[20] L. F. McGoldrick, O.M. Phillips, N. E. Huang, T. H. Hodgson, *Measurement on resonant wave interactions*, Journal of Fluid Mechanics, vol. 25, p. 437-456 (1966).

[21] L. F. McGoldrick, *On Wilton's ripples: a special case of resonant interactions*, Journal of Fluid Mechanics, vol. 42, part 1, p. 193-200 (1970).

[22] O. M. Phillips, *On the dynamics of unsteady gravity waves of finite amplitude. Part 1. The elementary interactions*, Journal of Fluid Mechanics, vol. 9, p. 193-217 (1960).

[23] O. M. Phillips, *Wave interactions - the evolution of an idea*, Journal of Fluid Mechanics, vol. 106, p. 215-227 (1981).

[24] H. Segur, *Resonant wave interactions of surface and internal gravity waves*, Physics of Fluids, vol. 23, p. 2556-2557 (1980).

[25] W. F. Simmons, *A Variational Method for Weak Resonant Wave Interactions*, Proceedings of the Royal Society of London. Series A, Mathematical and Physical Sciences, vol. 309, no. 1499 (Apr. 22, 1969), pp. 551-575 + 577-579

[26] T. M. A. Taklo and W. Choi, *Group resonant interactions between surface and internal gravity waves in a two-layer system*, Journal of Fluid Mechanics, vol. 892, A14 (2020).

[27] M. Tanaka, K. Wakayama, *A numerical study on the energy transfer from surface waves to interfacial waves in a two-layer fluid system*, Journal of Fluid Mechanics, vol. 763, p. 202-217 (2015).

[28] WJ. R. Wilton, *On Ripples*, Philosophical Magazine, Series 6, vol. 29 (173), p. 688-700 (1915).

[29] V. E. Zakharov, *Stability of periodic waves of finite amplitude on the surface of a deep fluid*, J. Applied Mech. Tech. Phys. vol. 9, p. 190-194 (1968).